Single top quark production via SUSY-QCD FCNC couplings at the CERN LHC in the unconstrained MSSM

Jian Jun Liu[a], Chong Sheng Li[a]*, Li Lin Yang[a] and Li Gang Jin[b]

[a] Department of Physics, Peking University, Beijing 100871, China

[b] Institute of Theoretical Physics, Academia Sinica, P. O. Box 2735, Beijing 100080, China

February 1, 2008

Abstract

We evaluate the $t\bar{c}$ and $t\bar{u}$ productions at the LHC within the general unconstrained MSSM framework. We find that these single top quark productions induced by SUSY-QCD FCNC couplings have remarkable cross sections for favorable parameter values allowed by current low energy data, which can be as large as a few pb. Once large rates of the $t\bar{c}$ and $t\bar{u}$ productions are detected at the LHC, they may be induced by SUSY FCNC couplings. We show that the precise measurement of single top quark production cross sections at the LHC is a powerful probe for the details of the SUSY FCNC couplings.

Keywords: top quark, MSSM, FCNC

PACS numbers: 14.65.Ha, 12.60.Jv, 11.30.pb

*csli@pku.edu.cn

1 Introduction

The flavor dynamics, such as the mixing of three generation fermions and their large mass differences observed, is still a great mystery in particle physics today. The heaviest one of three generation fermions is the top quark with the mass close to the electroweak (EW) symmetry breaking scale. Therefore, it can play a role of a wonderful probe for the EW breaking mechanism and new physics beyond the standard model (SM) through its decays and productions. An important aspect of the top quark physics is to investigate anomalous flavor changing neutral current (FCNC) couplings. Within the SM, FCNC is forbidden at the tree-level and highly suppressed by the GIM mechanism [1] at one-loop level. All the precise measurements of various FCNC processes, for example, $b \to s\gamma$ [2], agree with the SM predictions. However, many new physics models allow the existence of the tree-level FCNC couplings, and may enhance some FCNC processes. In particular, the minimal supersymmetric standard model (MSSM) is one of the most popular new physics models. And it is hard to believe that this model will say no more about the flavor dynamics than the SM. The MSSM includes 105 free parameters beyond the SM: 5 real parameters and 3 CP-violating phases in the gaugino/higgsino sector, 21 squark and slepton masses, 36 new real mixing angles to define the squark and slepton mass eigenstates, and 40 new CP-violating phases that can appear in squark and slepton interactions [2], so in general, it can provide a new explanation of the source of FCNC couplings. Actually, many of the parameters are constrained by present experimental data, and some popular SUSY models, for example, the gravity-mediated supersymmetry broken model (SUGRA) [3], gauge mediated supersymmetry broken model (GMSB) [4], anomaly mediated supersymmetry broken model (AMSB) [5], gaugino mediated supersymmetry broken model (gMSB) [6] and Kaluza-Klein mediated supersymmetry broken model [7], make some ad hoc assumptions to reduce the number of independent parameters. Although the predictions of these models can agree with the present constraints from FCNC experiments, it should be noted that few experimental constraints on the top quark FCNC processes are available so far [2]. Since the CERN Large Hadron Collider (LHC) can produce abundant top events, the measurement of the top quark rare processes will become possible. Therefore, a good un-

derstanding of the theoretical predictions of these processes, especially within the general unconstrained MSSM framework, is important. And a careful investigation will provide some clues to the constraint relations among the supersymmetry (SUSY) parameters and more clear information about the SUSY breaking mechanisms.

The top quark FCNC processes have been investigated in detail. There are two categories of these investigations, one of which is the top quark FCNC decays [8], especially for $t \to cg$ [9, 10] and $t \to ch$ [11] in the MSSM. These results show that the branch ratio of $t \to cg$ can reach 10^{-4} [10], which enhances the one in the SM ($\sim 10^{-11}$) significantly. The other category is the top quark productions through FCNC processes [12]–[17], ones of which induced by the anomalous top quark FCNC couplings at the colliders have been extensively discussed in a model independent way [12]–[16] and model dependent way [17], respectively. As we know, most of the works within SUSY models are limited in some constrained MSSM, where the top quark FCNC couplings were studied through some SUSY-CKM matrices or mass insertion approximation [18]. However, it is interesting to study the top quark FCNC productions using soft SUSY broken parameters directly, and then establish some relations between the production cross sections and soft SUSY broken parameters in the mass eigenstate formalism [19, 20]. Actually, the general framework with SUSY FCNC mechanisms was presented several years ago [21], and there have been a lot of works studying SUSY FCNC processes within this framework [19, 20]. But the top quark SUSY FCNC production processes have not been studied in above framework so far, and this means that the relations between the observables of the top quark production processes and the mixing among up squarks involving the third generation have not been established yet. In this paper, we will investigate the single top quark productions at the LHC induced by SUSY FCNC couplings in the general unconstrained MSSM, which include the top quark productions associated with the anti-charm quark and the anti-up quark, and we believe that it is an important step towards revealing the top quark SUSY FCNC couplings and exploring some relations among SUSY broken parameters at the LHC.

The paper is organized as follows: In Sec. 2 we describe the general framework of

SUSY FCNC mechanisms. In Sec. 3 we evaluate the total production cross sections of the $pp \to t\bar{c}(\bar{u})$ process induced by SUSY FCNC couplings, and the detail expressions for various couplings and form factors are given in the Appendices A and B, respectively. In Sec. 4 we present our numerical calculations and discussions. Finally, Sec. 5 gives our conclusions.

2 The FCNC in the MSSM

In order to make our paper self-contained, we start with a brief description of the FCNC mechanism in the MSSM, as shown in Ref. [21], and establish our notation conventions.

The SUSY part of the MSSM Lagrangian is

$$\begin{aligned}\mathcal{L}_{SUSY} &= -\frac{1}{4}F_G^{a\,\mu\nu}F_{G\,\mu\nu}^a + i\bar{\lambda}_G^a \not{D}_{ab}\lambda_G^b + (D^\mu\phi)^\dagger(D_\mu\phi) + i\bar{\psi}\not{D}\psi \\ &\quad -\left(\frac{\partial\tilde{\mathcal{W}}}{\partial\phi_i}\right)^\star\left(\frac{\partial\tilde{\mathcal{W}}}{\partial\phi_i}\right) - \frac{1}{2}\left(\frac{\partial^2\tilde{\mathcal{W}}}{\partial\phi_i\partial\phi_j}\psi_i^T C\psi_j \;+\; \text{h.c.}\right) \\ &\quad -\sqrt{2}g_G\left(\phi^\dagger T_G^a\lambda_G^{a\,T}C\psi \;+\; \text{h.c.}\right) - \frac{1}{2}g_G^2(\phi^\dagger T_G^a\phi)(\phi^\dagger T_G^a\phi), \qquad (1)\end{aligned}$$

where

$$\tilde{\mathcal{W}} = \mu H^1H^2 + Y_l^{IJ}H^1\tilde{L}^I\tilde{E}_R^J + Y_d^{IJ}H^1\tilde{Q}^I\tilde{D}_R^J + Y_u^{IJ}H^2\tilde{Q}^I\tilde{U}_R^J. \qquad (2)$$

Here the subscript G represents color, weak isospin and supercharge indices of the SM gauge group $SU(3)_C \times SU(2)_L \times U(1)_Y$, respectively, a and b are the indices of adjoint representations of the non-abelian subgroups, and $I, J = 1, 2, 3$ are the generation indices. ϕ, ψ and λ represent scalar fields, matter fermion fields and gauginos, respectively. C is charge conjugation matrix. $\tilde{L}^I(\tilde{Q}^I)$ and $\tilde{E}_R^I(\tilde{U}_R^I, \tilde{D}_R^I)$ represent slepton(squark) $SU(2)$ left-hand doublets and right-hand singlets, respectively. $H^{1,2}$ represent two Higgs $SU(2)$ doublets, and their vacuum expectation values are

$$\langle H^1\rangle = \begin{pmatrix} \frac{v_1}{\sqrt{2}} \\ 0 \end{pmatrix} \equiv \begin{pmatrix} \frac{v\cos\beta}{\sqrt{2}} \\ 0 \end{pmatrix}, \qquad \langle H^2\rangle = \begin{pmatrix} 0 \\ \frac{v_2}{\sqrt{2}} \end{pmatrix} \equiv \begin{pmatrix} 0 \\ \frac{v\sin\beta}{\sqrt{2}} \end{pmatrix}, \qquad (3)$$

where $v = (\sqrt{2}G_F)^{-1/2} = 246$ GeV, and the angle β is defined by $\tan\beta \equiv v_2/v_1$, the ratio of the vacuum expectation values of the two Higgs doublets. μ is the Higgs mixing parameter.

The soft SUSY breaking Lagrangian is

$$\begin{aligned}\mathcal{L}_{soft} &= -\frac{1}{2}\left(M_3\tilde{g}^{a\,T}C\tilde{g}^a + M_2\tilde{W}^{i\,T}C\tilde{W}^i + M_1\tilde{B}^TC\tilde{B} \;+\; \text{h.c.}\right) \\ &\quad -M_{H^1}^2 H^{1\,\dagger}H^1 - M_{H^2}^2 H^{2\,\dagger}H^2 - \tilde{L}^{I\dagger}(M_L^2)^{IJ}\tilde{L}^J - \tilde{E}_R^{I\dagger}(M_E^2)^{IJ}\tilde{E}_R^J \\ &\quad -\tilde{Q}^{I\dagger}(M_Q^2)^{IJ}\tilde{Q}^J - \tilde{D}_R^{I\dagger}(M_D^2)^{IJ}\tilde{D}_R^J - \tilde{U}_R^{I\dagger}(M_U^2)^{IJ}\tilde{U}_R^J \\ &\quad +\left(A_E^{IJ}H^1\tilde{L}^I\tilde{E}_R^J + A_D^{IJ}H^1\tilde{Q}^I\tilde{D}_R^J + A_U^{IJ}H^2\tilde{Q}^I\tilde{U}_R^J + B\mu H^1H^2 \;+\; \text{h.c.}\right). \end{aligned} \tag{4}$$

Here M_Q^2, $M_{U,D}^2$ and $A_{U,D}$ are the soft broken $SU(2)$ doublet squark mass squared matrix, the $SU(2)$ singlet squark mass squared matrix and the trilinear coupling matrix, respectively.

Using 3×3 unitary matrices $V_{L,R}^{E,U,D}$, the lepton and quark mass eigenstates are given by

$$\begin{aligned} \nu &= V_L^E\Psi_{L1}, & u &= V_L^U\Psi_{Q1} \;+\; V_R^UC\bar{\Psi}_U^T, \\ l &= V_L^E\Psi_{L2} \;+\; V_R^EC\bar{\Psi}_E^T, & d &= V_L^D\Psi_{Q2} \;+\; V_R^DC\bar{\Psi}_D^T. \end{aligned} \tag{5}$$

Their corresponding diagonal 3×3 mass matrices are

$$m_l = -\frac{v\cos\beta}{\sqrt{2}}V_R^EY_l^TV_L^{E\,\dagger}, \quad m_u = \frac{v\sin\beta}{\sqrt{2}}V_R^UY_u^TV_L^{U\,\dagger}, \quad m_d = -\frac{v\cos\beta}{\sqrt{2}}V_R^DY_d^TV_L^{D\,\dagger}.$$

As in the SM, the Cabbibo-Kobayashi-Maskawa (CKM) matrix is $K = V_L^UV_L^{D\,\dagger}$.

It is convenient to specify the squark mass matrices in the super-CKM basis, in which the mass matrices of the quark fields are diagonalized by rotating the superfields. The super-CKM basis $\tilde{U}^0$ is defined as

$$\tilde{U}^0 = \begin{pmatrix} V_L^U\tilde{U}_L \\ V_R^U\tilde{U}_R^* \end{pmatrix}. \tag{6}$$

And in this basis, the up squark mass matrix is 6×6 matrix, which has the form:

$$\mathcal{M}_{\tilde{U}}^2 \equiv \begin{pmatrix} \left(M_{\tilde{U}}^2\right)_{LL} + F_{u\,LL} + D_{u\,LL} & \left(M_{\tilde{U}}^2\right)_{LR} + F_{u\,LR} \\ \left(M_{\tilde{U}}^2\right)_{LR}^{\dagger} + (F_{u\,LR})^{\dagger} & \left(M_{\tilde{U}}^2\right)_{RR} + F_{u\,RR} + D_{u\,RR} \end{pmatrix}. \tag{7}$$

The F terms and D terms are diagonal 3×3 submatrices, which are given by

$$F_{u\,LR} = -\mu(m_u\cot\beta)\,\mathbb{1}_3\,, \qquad F_{u\,LL} = F_{u\,RR} = m_u^2\,\mathbb{1}_3\,, \tag{8}$$

$$D_{u\,LL} = D_{u\,RR} = \cos 2\beta\, m_Z^2 \left(\frac{1}{2} - \frac{2}{3}\sin^2\theta_W\right) \mathbb{1}_3\,, \tag{9}$$

where θ_W is the Weinberg angle, $\mathbb{1}_3$ stands for the 3×3 unit matrix. And $(M^2_{\tilde{U}})_{LL}$, $(M^2_{\tilde{U}})_{RR}$ and $(M^2_{\tilde{U}})_{LR}$ contain the flavor-changing entries

$$(M^2_{\tilde{U}})_{LL} = V_L^U M_Q^2 V_L^{U\dagger}, \qquad (M^2_{\tilde{U}})_{RR} = V_R^U (M_U^2)^T V_R^{U\dagger}, \qquad (M^2_{\tilde{U}})_{LR} = -\tfrac{v\sin\beta}{\sqrt{2}} V_L^U A_U^* V_R^{U\dagger}, \tag{10}$$

which are directly related to the mechanism of SUSY breaking, and are in general not diagonal in the super-CKM basis. Furthermore, $(M^2_{\tilde{U}})_{LR}$, arising from the trilinear terms in the soft potential, is not hermitian. The matrix $\mathcal{M}^2_{\tilde{U}}$ can further be diagonalized by an additional 6×6 unitary matrix Z_U to give the up squark mass eigenvalues

$$\left(\mathcal{M}^2_{\tilde{U}}\right)^{diag} = Z_U^\dagger \mathcal{M}^2_{\tilde{U}} Z_U. \tag{11}$$

As for the down squark mass matrix, we also can define $\mathcal{M}^2_{\tilde{D}}$ as the similar form of Eq. (7) with the replacement of $(M^2_{\tilde{U}})_{IJ}$ $(I,J = L,R)$ by $(M^2_{\tilde{D}})_{IJ}$. Note that since $SU(2)_L$ gauge invariance implies that $(M^2_{\tilde{U}})_{LL} = K(M^2_{\tilde{D}})_{LL}K^\dagger$, the matrices $(M^2_{\tilde{U}})_{LL}$ and $(M^2_{\tilde{D}})_{LL}$ are correlated and cannot be specified independently.

Thus, in the super-CKM basis, there are new potential sources of flavor-changing neutral current: neutralino-quark-squark coupling and gluino-quark-squark coupling, which arise from the off-diagonal elements of $(M^2_{\tilde{U}})_{LL}$, $(M^2_{\tilde{U}})_{LR}$ and $(M^2_{\tilde{U}})_{RR}$. As the former coupling is in general much weaker than the latter one, in this paper, we only consider the SUSY-QCD FCNC effects induced by the gluino-quark-squark coupling, which can be written as

$$i\sqrt{2}g_s T^a \left[-(Z_U)_{Ii} P_L + (Z_U)_{(I+3)i} P_R\right] \qquad I,i = 1,2,3. \tag{12}$$

Here $P_{L,R} \equiv (1\mp\gamma_5)/2$ and T^a is the $SU(3)$ color matrix. Thus the flavor changing effects of soft broken terms M_Q^2, M_U^2 and A_U on the observables can be obtained through the matrix Z_U.

As mentioned in the introduction, most of previous literatures studied the FCNC processes in the MSSM by so-called mass insertion approximation [18]. However, when the off-diagonal elements in the up squark mass matrix become large, the mass insertion

approximation is no longer valid [19, 20]. Therefore, we use the general mass eigenstate formalism as described above, which has been adopted in the literatures recently [10, 19, 20]. So any effects of SUSY FCNC couplings in loops on various observables will provide some information of the SUSY breaking mechanism.

In practical calculations, because the squark mass matrix $\mathcal{M}^2_{\tilde{U}}$ is a 6×6 matrix, it is very formidable to calculate the effects arising from the matrix on the observables of FCNC processes. Thus, as shown in Ref. [10, 19, 20], it is reasonable to calculate the observables by only switching on *one* off-diagonal element in $(M^2_{\tilde{U}})_{LL}$, $(M^2_{\tilde{U}})_{LR}$ and $(M^2_{\tilde{U}})_{RR}$ at a time. For the aim of this paper, the following strategy in the calculations of the process $pp \to t\bar{c}(\bar{u})$ will be used: first we deal with the LL, LR, RL and RR block of the matrix $\mathcal{M}^2_{\tilde{U}}$ separately and in each block we only consider the effects of individual element on the production cross sections, and then we investigate both the interference effects between different entries within one block and the interference effects between different blocks. To simplify the calculation we further assume that all diagonal entries in $(M^2_{\tilde{U}})_{LL}$, $(M^2_{\tilde{U}})_{LR}$, $(M^2_{\tilde{U}})_{RL}$ and $(M^2_{\tilde{U}})_{RR}$ are set to be equal to the common value $M^2_{\rm SUSY}$, and then we normalize the off-diagonal elements to $M^2_{\rm SUSY}$ [19, 22],

$$
\begin{aligned}
(\delta^{ij}_U)_{LL} &= \frac{(M^2_{\tilde{U}})^{ij}_{LL}}{M^2_{\rm SUSY}}\,, \qquad (\delta^{ij}_U)_{RR} = \frac{(M^2_{\tilde{U}})^{ij}_{RR}}{M^2_{\rm SUSY}}\,, \\
(\delta^{ij}_U)_{LR} &= \frac{(M^2_{\tilde{U}})^{ij}_{LR}}{M^2_{\rm SUSY}}\,, \qquad (\delta^{ij}_U)_{RL} = \frac{(M^2_{\tilde{U}})^{ij}_{RL}}{M^2_{\rm SUSY}}\,, \qquad (i \neq j, i, j = 1, 2, 3). \qquad (13)
\end{aligned}
$$

Thus $(M^2_{\tilde{U}})_{LL}$ can be written as follows:

$$
(M^2_{\tilde{U}})_{LL} = M^2_{\rm SUSY} \begin{pmatrix} 1 & (\delta^{12}_U)_{LL} & (\delta^{13}_U)_{LL} \\ (\delta^{21}_U)_{LL} & 1 & (\delta^{23}_U)_{LL} \\ (\delta^{31}_U)_{LL} & (\delta^{32}_U)_{LL} & 1 \end{pmatrix}, \qquad (14)
$$

and analogously for all the other blocks.

3 The process $pp \to t\bar{c}(\bar{u})$ induced by SUSY FCNC couplings

The process $pp \to t\bar{c}(\bar{u})$ at the LHC can be induced through the SUSY-QCD FCNC couplings with the initial partonic states $u\bar{u}$, $d\bar{d}$, $s\bar{s}$, $c\bar{c}$, $u\bar{c}$, $c\bar{u}$ and gg, as shown in Fig.1. Our practical calculations show that the contributions from the $b\bar{b}$, $b\bar{s}$ and $s\bar{b}$ initial states are negligibly small, so we do not discuss them below. As the $t\bar{u}$ process is completely similar to the $t\bar{c}$ one, here we only discuss the situations of $t\bar{c}$ in detail. Neglecting the charm quark mass, the amplitude of the process $gg \to t\bar{c}$ can be written as

$$\mathcal{M}^{gg} = \mathcal{M}^{gg}_{self} + \mathcal{M}^{gg}_{vertex} + \mathcal{M}^{gg}_{box}, \tag{15}$$

where $\mathcal{M}^{gg}_{self}$, $\mathcal{M}^{gg}_{vertex}$ and $\mathcal{M}^{gg}_{box}$ are the amplitudes of self-energy diagrams Figs.1(a)–(e), vertex diagrams Figs.1(f), (g) and (h) and box diagrams Figs.1(i)–(o), respectively. They can be further expressed as

$$\mathcal{M}^{gg}_{self} = \sum_{i=1}^{14} f^i_s \mathcal{M}^{gg}_i \ , \tag{16}$$

$$\mathcal{M}^{gg}_{vertex} = \sum_{i=1}^{30} f^i_v \mathcal{M}^{gg}_i \ , \tag{17}$$

and

$$\mathcal{M}^{gg}_{box} = \sum_{i=1}^{40} f^i_b \mathcal{M}^{gg}_i \ , \tag{18}$$

respectively. Here f^i_s, f^i_v and f^i_b are form factors corresponding to the self-energy diagrams, vertex diagrams and box diagrams, respectively, and their expressions are given explicitly in Appendix B. $\mathcal{M}^{gg}_i$ are the standard matrix elements, which are defined by

$$\begin{aligned}
\mathcal{M}^{gg}_{1,2} &= \bar{u}(p_t) \not{\varepsilon}(k_1) k_1 \cdot \varepsilon(k_2) P_{L,R} v(p_c), \\
\mathcal{M}^{gg}_{3,4} &= \bar{u}(p_t) \not{\varepsilon}(k_2) k_2 \cdot \varepsilon(k_1) P_{L,R} v(p_c), \\
\mathcal{M}^{gg}_{5,6} &= \bar{u}(p_t) \not{\varepsilon}(k_2) p_t \cdot \varepsilon(k_1) P_{L,R} v(p_c), \\
\mathcal{M}^{gg}_{7,8} &= \bar{u}(p_t) \not{k}_1 \varepsilon(k_1) \cdot \varepsilon(k_2) P_{L,R} v(p_c),
\end{aligned}$$

$$
\begin{aligned}
\mathcal{M}^{gg}_{9,10} &= \bar{u}(p_t)\varepsilon(k_1)\cdot\varepsilon(k_2)P_{L,R}v(p_c),\\
\mathcal{M}^{gg}_{11,12} &= \bar{u}(p_t)\ \not{\varepsilon}(k_1)\ \not{k}_1\ \not{\varepsilon}(k_2)P_{L,R}v(p_c),\\
\mathcal{M}^{gg}_{13,14} &= \bar{u}(p_t)\ \not{\varepsilon}(k_1)\ \not{\varepsilon}(k_2)P_{L,R}v(p_c),\\
\mathcal{M}^{gg}_{15,16} &= \bar{u}(p_t)\ \not{\varepsilon}(k_1)\ \not{k}_1 k_1\cdot\varepsilon(k_2)P_{L,R}v(p_c),\\
\mathcal{M}^{gg}_{17,18} &= \bar{u}(p_t)\ \not{\varepsilon}(k_1)p_t\cdot\varepsilon(k_2)P_{L,R}v(p_c),\\
\mathcal{M}^{gg}_{19,20} &= \bar{u}(p_t)\ \not{\varepsilon}(k_1)\ \not{k}_1 p_t\cdot\varepsilon(k_2)P_{L,R}v(p_c),\\
\mathcal{M}^{gg}_{21,22} &= \bar{u}(p_t)\ \not{\varepsilon}(k_2)\ \not{k}_1 k_2\cdot\varepsilon(k_1)P_{L,R}v(p_c),\\
\mathcal{M}^{gg}_{23,24} &= \bar{u}(p_t)\ \not{\varepsilon}(k_2)\ \not{k}_1 p_t\cdot\varepsilon(k_1)P_{L,R}v(p_c),\\
\mathcal{M}^{gg}_{25,26} &= \bar{u}(p_t)k_1\cdot\varepsilon(k_2)p_t\cdot\varepsilon(k_1)P_{L,R}v(p_c),\\
\mathcal{M}^{gg}_{27,28} &= \bar{u}(p_t)p_t\cdot\varepsilon(k_2)k_2\cdot\varepsilon(k_1)P_{L,R}v(p_c),\\
\mathcal{M}^{gg}_{29,30} &= \bar{u}(p_t)p_t\cdot\varepsilon(k_2)p_t\cdot\varepsilon(k_1)P_{L,R}v(p_c),\\
\mathcal{M}^{gg}_{31,32} &= \bar{u}(p_t)\ \not{k}_1 k_1\cdot\varepsilon(k_2)k_2\cdot\varepsilon(k_1)P_{L,R}v(p_c),\\
\mathcal{M}^{gg}_{33,34} &= \bar{u}(p_t)\ \not{k}_1 k_1\cdot\varepsilon(k_2)p_t\cdot\varepsilon(k_1)P_{L,R}v(p_c),\\
\mathcal{M}^{gg}_{35,36} &= \bar{u}(p_t)k_1\cdot\varepsilon(k_2)k_2\cdot\varepsilon(k_1)P_{L,R}v(p_c),\\
\mathcal{M}^{gg}_{37,38} &= \bar{u}(p_t)\ \not{k}_1 p_t\cdot\varepsilon(k_2)k_2\cdot\varepsilon(k_1)P_{L,R}v(p_c),\\
\mathcal{M}^{gg}_{39,40} &= \bar{u}(p_t)\ \not{k}_1 p_t\cdot\varepsilon(k_2)p_t\cdot\varepsilon(k_1)P_{L,R}v(p_c),
\end{aligned}
\tag{19}
$$

where $k_{1,2}$ denote the momenta of incoming partons, while p_t and p_c are used for the outgoing top and anti-charm quarks, respectively.

For the quarks initiated subprocesses, we also define the standard matrix elements as

$$
\begin{aligned}
\mathcal{M}^{q'\bar{q}}_{1\alpha\beta} &= \bar{v}(k_2)P_\alpha\gamma_\mu u(k_1)\bar{u}(p_t)P_\beta\gamma^\mu v(p_c),\\
\mathcal{M}^{q'\bar{q}}_{2\alpha\beta} &= \bar{u}(p_t)P_\alpha v(p_c)\bar{v}(k_2)P_\beta\not{p}_t u(k_1),\\
\mathcal{M}^{q'\bar{q}}_{3\alpha\beta} &= \bar{v}(k_2)P_\alpha u(k_1)\bar{u}(p_t)P_\beta v(p_c),\\
\mathcal{M}^{q'\bar{q}}_{4\alpha\beta} &= \bar{v}(k_2)P_\alpha u(k_1)\bar{u}(p_t)P_\beta\not{k}_1 v(p_c),\\
\mathcal{M}^{q'\bar{q}}_{5\alpha\beta} &= \bar{v}(k_2)P_\alpha v(p_c)\bar{u}(p_t)P_\beta u(k_1),\\
\mathcal{M}^{q'\bar{q}}_{6\alpha\beta} &= \bar{v}(k_2)P_\alpha v(p_c)\bar{u}(p_t)P_\beta\not{k}_2 u(k_1),\\
\mathcal{M}^{q'\bar{q}}_{7\alpha\beta} &= \bar{u}(p_t)P_\alpha u(k_1)\bar{v}(k_2)P_\beta\not{k}_1 v(p_c),
\end{aligned}
$$

$$\mathcal{M}^{q'\bar{q}}_{8\alpha\beta} = \bar{v}(k_2)P_\alpha \not{k}_1 v(p_c)\bar{u}(p_t)P_\beta \not{k}_2 u(k_1),$$
$$\mathcal{M}^{q'\bar{q}}_{9\alpha\beta} = \bar{v}(k_2)P_\alpha \not{p}_t u(k_1)\bar{u}(p_t)P_\beta \not{k}_1 v(p_c),$$
$$\mathcal{M}^{q'\bar{q}}_{10\alpha\beta} = \bar{v}(k_2)P_\alpha \gamma_\mu v(p_c)\bar{u}(p_t)P_\beta \gamma^\mu u(k_1),$$
$$\mathcal{M}^{q'\bar{q}}_{11\alpha\beta} = \bar{u}(p_t)P_\alpha u(k_2)\bar{v}(p_c)P_\beta v(k_1),$$
$$\mathcal{M}^{q'\bar{q}}_{12\alpha\beta} = \bar{u}(p_t)P_\alpha u(k_2)\bar{v}(p_c)P_\beta \not{k}_2 v(k_1),$$
$$\mathcal{M}^{q'\bar{q}}_{13\alpha\beta} = \bar{u}(p_t)P_\beta \not{k}_1 u(k_2)\bar{v}(p_c)P_\alpha v(k_1),$$
$$\mathcal{M}^{q'\bar{q}}_{14\alpha\beta} = \bar{u}(p_t)P_\alpha \not{k}_1 u(k_2)\bar{v}(p_c)P_\beta \not{k}_2 v(k_1),$$
$$\mathcal{M}^{q'\bar{q}}_{15\alpha\beta} = \bar{u}(p_t)P_\alpha \gamma_\mu u(k_2)\bar{v}(p_c)P_\beta \gamma^\mu v(k_1), \tag{20}$$

where (α,β)=(L,L), (L,R), (R,L) and (R,R), respectively. And the amplitude for the quarks initiated subprocesses can be expressed as

$$\mathcal{M}^{q'\bar{q}} = \sum_{i=1}^{15} \sum_{\alpha,\beta=L,R} g^{i\alpha\beta}\mathcal{M}^{q'\bar{q}}_{i\alpha\beta}, \tag{21}$$

where the $g^{i\alpha\beta}$ are form factors which can be fixed by the straightforward calculations of the relevant diagrams. However, the Feynman diagrams contributing to the subprocesses with the different initial states can be different. We first describe the amplitude of the subprocess $c\bar{c} \to t\bar{c}$, which has the largest set of Feynman diagrams, i.e. all diagrams in Fig.2, and the explicit expressions of the non-zero $g^{i\alpha\beta}$ of each diagram can be found in Appendix B. In Table 1 we list all other channels that can contribute to $t\bar{c}(\bar{u})$ production and their related Feynman diagrams, and their corresponding form factors can be obtained from ones of $c\bar{c} \to t\bar{c}$ by modifying some couplings as shown in the Table.

The partonic level cross section for $\kappa\lambda \to t\bar{c}$ is

$$\hat{\sigma}^{\kappa\lambda} = \int_{\hat{t}_-}^{\hat{t}_+} \frac{1}{16\pi\hat{s}^2}\overline{\sum}|\mathcal{M}^{\kappa\lambda}|^2 d\hat{t} \tag{22}$$

with

$$\hat{t}_\pm = \frac{m_c^2 + m_t^2 - \hat{s}}{2} \pm \frac{1}{2}\sqrt{(\hat{s} - (m_c + m_t)^2)(\hat{s} - (m_c - m_t)^2)}, \tag{23}$$

where $\sqrt{\hat{s}}$ is the c.m. energy of the $\kappa\lambda$ (gg or $q'\bar{q}$) states. The total hadronic cross section for $pp \to \kappa\lambda \to t\bar{c}$ can be written in the form

$$\sigma(s) = \sum_{\kappa,\lambda} \int_{(m_c+m_t)/\sqrt{s}}^1 dz \frac{dL}{dz}\hat{\sigma}^{\kappa\lambda}(\kappa\lambda \to t\bar{c} \ \text{ at } \ \hat{s} = z^2 s). \tag{24}$$

channel	related diagrams in Fig.2	form factors
$u\bar{u} \to t\bar{u}$	$b_1, b_2, b_3, b_4, v_1, v_2, v_3, v_4, s_1, s_2, s_3, s_4$	$g_\rho^{i\alpha\beta}(V_{5L(R)} \leftrightarrow V_{4L(R)})$
$u\bar{u} \to t\bar{c}$	$b_1, b_2, b_3, b_4, v_1, v_2, s_1, s_2$	$g_\rho^{i\alpha\beta}(V_{5L(R)} \leftrightarrow V_{4L(R)})$
$c\bar{c} \to t\bar{u}$		$g_\rho^{i\alpha\beta}(V_{5L(R)} \leftrightarrow V_{4L(R)})$
$u\bar{c} \to t\bar{c}$	$b_1, b_2, b_3, b_4, v_3, v_4, s_3, s_4$	$g_\rho^{i\alpha\beta}(V_{5L(R)} \leftrightarrow V_{4L(R)})$
$c\bar{u} \to t\bar{u}$		$g_\rho^{i\alpha\beta}(V_{5L(R)} \leftrightarrow V_{4L(R)})$
$c\bar{u} \to t\bar{c}$	b_1, b_2, b_3, b_4	$g_\rho^{i\alpha\beta}(V_{5L(R)} \leftrightarrow V_{4L(R)})$
$u\bar{c} \to t\bar{u}$		$g_\rho^{i\alpha\beta}(V_{5L(R)} \leftrightarrow V_{4L(R)})$
$s\bar{s} \to t\bar{c}(\bar{u})$	$b_2, b_3, v_1, v_2, s_1, s_2$	$g_\rho^{i\alpha\beta}(V_{6L(R)} \leftrightarrow V_{5L(R)})$
$d\bar{d} \to t\bar{c}(\bar{u})$		$g_\rho^{i\alpha\beta}(V_{6L(R)} \leftrightarrow V_{4L(R)})$

Table 1: The form factors of other channels obtained from ones of $c\bar{c} \to t\bar{c}$. Here, $V_{iL(R)}$ are defined in the Appendix A. The subscript ρ represents the corresponding diagram.

Here $\sqrt{s}$ is the c.m. energy of the pp states, and dL/dz is the parton luminosity, defined as

$$\frac{dL}{dz} = 2z \int_{z^2}^1 \frac{dx}{x} f_{\kappa/p}(x,\mu) f_{\lambda/p}(z^2/x,\mu), \tag{25}$$

where $f_{\kappa/p}(x,\mu)$ and $f_{\lambda/p}(z^2/x,\mu)$ are the κ and λ parton distribution functions, respectively.

4 Numerical calculation and discussion

In the following we present some numerical results for the total cross section of the single top quark production induced by SUSY-QCD FCNC couplings at the LHC. In our numerical calculations the SM parameters were taken to be $m_t = 174.3$ GeV, $M_W = 80.423$ GeV, $M_Z = 91.1876$ GeV, $m_c = 1.2$ GeV, $\sin^2(\theta_W) = 0.23113$ and $\alpha_s(M_Z) = 0.1172$ [2]. And we used the CTEQ6L PDF [23] and took the factorization scale and the renormalization scale as $\mu_f = \mu_r = m_t/2$. The relevant SUSY parameters are μ, $\tan\beta$, $M_{\rm SUSY}$ and $m_{\tilde{g}}$, which are unrelated to flavor changing mechanism, and may be fixed from flavor conserv-

ing observables at the future colliders. And they are chosen as follows: $M_{\rm SUSY} = 400, 1000$ GeV, $\tan\beta = 3, 30$, $m_{\tilde{g}} = 200, 300$ GeV and $\mu = 200$ GeV. As for the range of the flavor mixing parameters, $(\delta_U^{ij})_{LL}$ are constrained by corresponding $(\delta_D^{ij})_{LL}$ [19, 22, 24, 25], in which $(\delta_U^{12})_{LL}$ also is constrained by K-$\bar{K}$ mixing [26], and D_0-$\bar{D}_0$ mixing makes constraints on $(\delta_U^{12})_{LL}$, $(\delta_U^{12})_{LR}$ and $(\delta_U^{12})_{RL}$ [27]. And $(\delta_U^{31})_{LL}$, $(\delta_U^{32})_{LL}$, $(\delta_U^{31})_{RL}$ and $(\delta_U^{32})_{RL}$ are constrained by the chargino contributions to B_d-$\bar{B}_d$ mixing [24]. Finally, there also are constraints on the up squark mass matrix from the chargino contributions to $b \to s\gamma$ [19, 28]. Taking into account above constraints, in our numerical calculations, we use the following limits:

(i) $(\delta_U^{12})_{LL}$, $(\delta_U^{12})_{LR}$ and $(\delta_U^{12})_{RL}$ are less than $0.08 M_{\rm SUSY}/(1\ {\rm TeV})$;

(ii) $(\delta_U^{12})_{RR}$ and $(\delta_U^{13})_{LL}$ are limited below $0.2 M_{\rm SUSY}/(1\ {\rm TeV})$;

(iii) $(\delta_U^{23})_{LL}$, $(\delta_U^{23})_{LR}$, $(\delta_U^{23})_{RL}$, $(\delta_U^{23})_{RR}$, $(\delta_U^{13})_{LR}$, $(\delta_U^{13})_{RL}$ and $(\delta_U^{13})_{RR}$ vary from 0 to 1.

Our results are shown in Figs. 3–10. There are two common features of these curves: one is that the cross sections increase rapidly with the mixing parameters increasing, and the other is that the cross sections depend strongly on the gluino mass $m_{\tilde{g}}$, but weakly depend on $\tan\beta$ (so we just discuss the results for $\tan\beta = 30$ below). Comparing with above cases, the dependence on $M_{\rm SUSY}$ is medium.

Fig. 3 shows that in general the production rates of gluon fusion processes are several times larger than ones of the $q\bar{q}'$ annihilation, and these rates all depend strongly on the gluino mass $m_{\tilde{g}}$. For example, assuming $(\delta_U^{13})_{LR} = 0.7$ and $\tan\beta = 30$, the production rates of $gg \to t\bar{u}$ decrease from 700 fb at $m_{\tilde{g}} = 200$ GeV to 70 fb at $m_{\tilde{g}} = 500$ GeV.

Fig. 4 shows the dependence of the cross sections on the (δ_U^{23}) in the LL block. For $\tan\beta = 30$ the cross section of $t\bar{c}$ production can reach around 12 fb when $(\delta_U^{23})_{LL} = 0.7$, $M_{\rm SUSY} = 400$ GeV, and $m_{\tilde{g}} = 200$ GeV, as shown in Fig.4(b), but for $t\bar{u}$ production it is one order of magnitude smaller. The production cross sections arising from $(\delta_U^{13})_{LL}$ are less than 1 fb as $(\delta_U^{13})_{LL}$ is limited below $0.2 M_{\rm SUSY}/(1\ {\rm TeV})$, so we do not show the corresponding curves here.

Figs. 5 and 6 give the cross sections as the functions of (δ_U^{13}) and (δ_U^{23}) in the RR block, respectively. We can see that the cross sections of $t\bar{u}$ production are larger than ones of

$t\bar{c}$ production for the case where $(\delta_U^{13})_{RR} \neq 0$ and all the other mixing parameters are set to be 0, and in contrast with this case, the cross sections of $t\bar{c}$ production are larger than ones of $t\bar{u}$ production for the case of $(\delta_U^{23})_{RR} \neq 0$. For example, assuming $\tan\beta = 30$, $M_{\rm SUSY} = 400$ GeV, and $m_{\tilde{g}} = 200$ GeV, the cross sections of $t\bar{c}$ and $t\bar{u}$ productions are 12 fb and 1fb for $(\delta_U^{23})_{RR} = 0.7$, respectively, but 2 fb and 13 fb for $(\delta_U^{13})_{RR} = 0.7$, respectively.

Figs. 7 and 8 show the dependence of the cross sections on (δ_U^{13}) and (δ_U^{23}) in the LR block, respectively. We can see that the cross sections are much larger than ones arising from the mixing in the LL and RR blocks, which indicates that the SUSY FCNC effects induced by the mixing in the LR block can enhance the cross sections significantly. For example, for $\tan\beta = 30$, $M_{\rm SUSY} = 400$ GeV, and $m_{\tilde{g}} = 200$ GeV, the cross section can reach 643 fb for $(\delta_U^{23})_{LR} = 0.7$, and 75 fb for $(\delta_U^{13})_{LR} = 0.7$, as shown in Fig.7(b) and 8(b), respectively. Here we see again that the production cross sections of $t\bar{c}$ and $t\bar{u}$ depend strongly on $(\delta_U^{23})_{LR}$ and $(\delta_U^{13})_{LR}$, respectively. The cases of the RL block are similar to ones of the LR block, so we do not show them here. From Figs. 7 and 8 we can find that the production rates may be as large as a few pb for favorable parameter values.

In the above discussion for Figs. 3-8, we only show the results for $m_{\tilde{g}} = 200$ GeV and $M_{\rm SUSY} = 400$ GeV, and the corresponding results for other cases ($m_{\tilde{g}} = 200$ GeV and $M_{\rm SUSY} = 1000$ GeV, $m_{\tilde{g}} = 300$ GeV and $M_{\rm SUSY} = 400$ or 1000 GeV) decrease significantly, but they are still remarkable and vary from a few fb to hundreds of fb.

In Figs. 9, we give the results to uncover the interference effects between different entries within one block and between different blocks for $t\bar{c}$ production. Figs. 9(a)-(b) show the typical interference effects between $(\delta_U^{13})_{LR}$ and $(\delta_U^{23})_{LR}$ within the LR block and between $(\delta_U^{13})_{RR}$ and $(\delta_U^{23})_{RR}$ within the RR block, respectively. Figs. 9(c)-(d) show the interference effects between the LL and LR block and between the LL and RR block for the typical parameters, respectively. In general, those interference effects enhance the cross sections. And the interference effects for $t\bar{u}$ production are very similar to the case of $t\bar{c}$ production and are shown in Fig. 10. Although the interference effects do not change the cross sections of single top quark production at the LHC significantly, the

consideration of them is of importance to reveal the details of flavor changing mechanism.

Finally, for convenience, we list some typical results in Table 2.

subprocess	$(\delta_U^{23})_{LL}$	$(\delta_U^{13})_{RR}$	$(\delta_U^{23})_{RR}$	$(\delta_U^{13})_{LR}$	$(\delta_U^{23})_{LR}$
$gg \to t\bar{u}$	0	14.4	0	650.4	0
$q\bar{q}' \to t\bar{u}$	0.2	4.7	0.2	124.1	12.6
$gg \to t\bar{c}$	11.0	0	10.5	0	633.0
$q\bar{q}' \to t\bar{c}$	1.6	1.8	1.5	74.5	10.0
total	12.8	20.9	12.2	849.0	655.6

Table 2: Cross sections in fb for the $t\bar{c}$ and $t\bar{u}$ productions. Here $\tan\beta = 30$, $M_{\rm SUSY} = 400$ GeV and $m_{\tilde{g}} = 200$ GeV, the off-diagonal element in the table equals to 0.7 and others are set to zero.

5 Conclusions

We have evaluated the $t\bar{c}$ and $t\bar{u}$ productions at the LHC within the general unconstrained MSSM framework. These single top quark productions are induced by SUSY-QCD FCNC couplings and have remarkable cross sections for favorable parameter values allowed by current low energy data, which can be as large as a few pb. It has been pointed out [13] that the top quark FCNC production signals are more accessible than the top quark FCNC decay signals. And according to the model independent analysis in Ref. [14], it is possible to observe FCNC effects through single top quark productions at the LHC. Thus, our above results show that once large rates of the $t\bar{c}$ and $t\bar{u}$ productions are detected at the LHC, they may be induced by SUSY FCNC couplings, and such flavor changing must come from the LR or RL block, which is related to the soft trilinear couplings A_U. Therefore, we believe that the precise measurement of single top quark production cross sections at the LHC is a powerful probe for the details of the SUSY FCNC couplings.

ACKNOWLEDGMENTS

This work was supported in part by the National Natural Science Foundation of China and Specialized Research Fund for the Doctoral Program of Higher Education.

A Couplings

Here we list the relevant couplings in the amplitudes. i, j stand for generation indices and r, s stand for color indices.

$$V_1 = -ig_sT^a \qquad V_2 = -g_sf_{abc} \qquad V_3 = -ig_sf_{abc} \tag{26}$$

$$V_{4L} = -i\sqrt{2}g_sT^a_{rs}Z^q_{3i} \quad V_{4R} = i\sqrt{2}g_sT^a_{rs}Z^q_{6i} \tag{27}$$

$$V_{5L} = -i\sqrt{2}g_sT^a_{rs}Z^q_{2i} \quad V_{5R} = i\sqrt{2}g_sT^a_{rs}Z^q_{5i} \tag{28}$$

$$V_{6L} = -i\sqrt{2}g_sT^a_{rs}Z^q_{1i} \quad V_{6R} = i\sqrt{2}g_sT^a_{rs}Z^q_{4i} \tag{29}$$

$$V_7 = i/2g_s^2(1/3\delta_{ab} + d_{abc}T^c) \tag{30}$$

B Form Factors

This appendix lists all the form factors in the amplitude of various subprocess of $pp \to t\bar{c}$, in terms of 2,3- and 4-points one-loop integrals [29]. For convenience, we define the abbreviations of one-loop integrals as following:

$$\begin{aligned}
B^a &= B(s, m^2_{\tilde{g}}, m^2_{\tilde{g}}) \\
B^d &= B(t, m^2_{\tilde{g}}, m^2_{\tilde{g}}) \\
B^t &= B(0, m^2_{\tilde{g}}, m^2_{\tilde{q}}) \\
B^q &= B(m^2_t, m^2_{\tilde{g}}, m^2_{\tilde{q}}) \\
B^g &= B(t, m^2_{\tilde{g}}, m^2_{\tilde{q}}) \\
B^m &= B(u, m^2_{\tilde{g}}, m^2_{\tilde{q}})
\end{aligned}$$

$$
\begin{aligned}
C &= C(m_t^2, s, 0, m_{\tilde{q}}^2, m_{\tilde{g}}^2, m_{\tilde{g}}^2) \\
C^d &= C(m_t^2, s, 0, m_{\tilde{g}}^2, m_{\tilde{q}}^2, m_{\tilde{q}}^2) \\
C^t &= C(m_t^2, t, 0, m_{\tilde{q}}^2, m_{\tilde{g}}^2, m_{\tilde{g}}^2) \\
C^q &= C(m_t^2, t, 0, m_{\tilde{g}}^2, m_{\tilde{q}}^2, m_{\tilde{q}}^2) \\
C^g &= C(0, m_t^2, s, m_{\tilde{g}}^2, m_{\tilde{q}}^2, m_{\tilde{g}}^2) \\
C^f &= C(m_t^2, 0, s, m_{\tilde{g}}^2, m_{\tilde{q}}^2, m_{\tilde{g}}^2) \\
C^m &= C(0, 0, t, m_{\tilde{q}}^2, m_{\tilde{q}}^2, m_{\tilde{g}}^2) \\
C^n &= C(0, 0, t, m_{\tilde{g}}^2, m_{\tilde{g}}^2, m_{\tilde{q}}^2) \\
C^l &= C(0, t, 0, m_{\tilde{g}}^2, m_{\tilde{g}}^2, m_{\tilde{q}}^2) \\
C^o &= C(0, t, 0, m_{\tilde{g}}^2, m_{\tilde{q}}^2, m_{\tilde{g}}^2) \\
C^p &= C(0, u, 0, m_{\tilde{g}}^2, m_{\tilde{q}}^2, m_{\tilde{g}}^2) \\
C^r &= C(0, u, 0, m_{\tilde{q}}^2, m_{\tilde{g}}^2, m_{\tilde{q}}^2) \\
C^x &= C(0, u, m_t^2, m_{\tilde{g}}^2, m_{\tilde{g}}^2, m_{\tilde{q}}^2) \\
C^y &= C(0, u, m_t^2, m_{\tilde{q}}^2, m_{\tilde{q}}^2, m_{\tilde{g}}^2) \\
C^z &= C(m_t^2, t, 0, m_{\tilde{g}}^2, m_{\tilde{q}}^2, m_{\tilde{g}}^2) \\
C^w &= C(m_t^2, t, 0, m_{\tilde{q}}^2, m_{\tilde{g}}^2, m_{\tilde{q}}^2) \\
D &= D(0, 0, m_t^2, 0, t, s, m_{\tilde{g}}^2, m_{\tilde{q}}^2, m_{\tilde{g}}^2, m_{\tilde{q}}^2) \\
D^v &= D(0, 0, m_t^2, 0, t, s, m_{\tilde{q}}^2, m_{\tilde{g}}^2, m_{\tilde{q}}^2, m_{\tilde{g}}^2) \\
D^t &= D(0, m_t^2, 0, 0, u, s, m_{\tilde{q}}^2, m_{\tilde{g}}^2, m_{\tilde{q}}^2, m_{\tilde{g}}^2) \\
D^q &= D(m_t^2, 0, 0, 0, u, t, m_{\tilde{q}}^2, m_{\tilde{g}}^2, m_{\tilde{q}}^2, m_{\tilde{q}}^2) \\
D^g &= D(0, 0, m_t^2, 0, t, s, m_{\tilde{g}}^2, m_{\tilde{g}}^2, m_{\tilde{q}}^2, m_{\tilde{g}}^2) \\
D^f &= D(0, 0, m_t^2, 0, t, s, m_{\tilde{q}}^2, m_{\tilde{q}}^2, m_{\tilde{g}}^2, m_{\tilde{q}}^2) \\
D^s &= D(0, m_t^2, 0, 0, u, s, m_{\tilde{g}}^2, m_{\tilde{g}}^2, m_{\tilde{q}}^2, m_{\tilde{g}}^2) \\
D^m &= D(0, m_t^2, 0, 0, u, s, m_{\tilde{q}}^2, m_{\tilde{q}}^2, m_{\tilde{g}}^2, m_{\tilde{q}}^2) \\
D^n &= D(m_t^2, 0, 0, 0, u, t, m_{\tilde{g}}^2, m_{\tilde{q}}^2, m_{\tilde{q}}^2, m_{\tilde{g}}^2) \\
D^l &= D(m_t^2, 0, 0, 0, u, s, m_{\tilde{q}}^2, m_{\tilde{g}}^2, m_{\tilde{g}}^2, m_{\tilde{q}}^2)
\end{aligned}
$$

Below we display the non-zero form factors for the gluon fusion subprocess (we only display the odd number form factors, and the even number ones can be obtained by the replacement of $V_{4L} \leftrightarrow V_{4R}$ and $V_{5L} \leftrightarrow V_{5R}$ correspondingly). For self-energy diagram (see Figs.1(a)–(e)), f_s^i are:

$$\begin{aligned}
f_s^1 &= \frac{1}{m_t^3\pi^2 s(m_t^2-t)t}(V_{4L}(m_{\tilde{g}}m_t^2 tB_0^t V_1 V_{5L}(sV_1+(t-m_t^2)V_3) \\
&\quad +m_t V_1(-B_0^g m_{\tilde{g}}m_t^3 sV_1V_{5L}+(m_t^2-t)(m_{\tilde{g}}m_t B_0^q V_{5R} \\
&\quad -B_1^q m_t^2 V_{5L})(sV_2+tV_3)+m_t^2 stV_1V_{5R}B_1^g))) \qquad (31)\\
f_s^3 &= \frac{1}{m_t^3\pi^2 s(m_t^2-t)t}(V_{4L}(-m_t(m_t^2-u)V_1(m_{\tilde{g}}m_t B_0^q V_{5R} \\
&\quad -B_1^q m_t^2 V_{5L})(uV_3-sV_1)-m_t^2 V_1(m_{\tilde{g}}B_0^t uV_{5L}((u-m_t^2)V_3 \\
&\quad -sV_2)+m_t sV_1(B_0^m m_{\tilde{g}}m_t V_{5L}-uV_{5R}B_1^m)))) \qquad (32)\\
f_s^5 &= \frac{1}{8\pi^2}(V_1V_{4L}(\frac{m_{\tilde{g}}B_0^t V_1V_{5L}}{m_t t-m_t^3}+\frac{m_{\tilde{g}}B_0^t V_2V_{5L}}{m_t u-m_t^3} \\
&\quad +\frac{V_1(B_1^q m_t^2 V_{5L}-m_{\tilde{g}}m_t B_0^q V_{5R})}{m_t^2 u}+\frac{V_2(B_1^q m_t^2 V_{5L}-m_{\tilde{g}}m_t B_0^q V_{5R})}{m_t^2 t} \\
&\quad +\frac{V_1(tV_{5R}B_1^g-B_0^g m_{\tilde{g}}m_t V_{5L})}{t(t-m_t^2)}+\frac{V_1(uV_{5R}B_1^m-B_0^m m_{\tilde{g}}m_t V_{5L})}{u(u-m_t^2)})) \qquad (33)\\
f_s^7 &= \frac{1}{m_t^3\pi^2 s(m_t^2-t)t}(V_{4R}(-m_t(m_t^2-u)V_1(m_{\tilde{g}}m_t B_0^q V_{5L} \\
&\quad -B_1^q m_t^2 V_{5R})(uV_3-sV_1)-m_t^2 V_1(m_{\tilde{g}}B_0^t uV_{5R}((u-m_t^2)V_3-sV_2) \\
&\quad +m_t sV_1(B_0^m m_{\tilde{g}}m_t V_{5R}-uV_{5L}B_1^m)))) \qquad (34)\\
f_s^9 &= \frac{1}{16m_t^2\pi^2 s(m_t^2-u)}(V_1V_{4R}(2m_{\tilde{g}}m_t^2 s(B_0^m V_1-B_0^t V_2)V_{5R}-(m_t^2-u)(B_1^q V_{5R}m_t^3 \\
&\quad -m_{\tilde{g}}m_t^2 B_0^q V_{5L}+m_{\tilde{g}}m_t^2 B_0^t V_{5R})V_3-2m_t^3 sV_1V_{5L}B_1^m)) \qquad (35)\\
f_s^{11} &= \frac{1}{2}f_s^5 \qquad (36)\\
f_s^{13} &= \frac{1}{16m_t^2\pi^2 t(t-m_t^2)(m_t^2-u)}(V_{4R}((m_t^2-u)V_1V_2(B_1^q m_t^3 V_{5R}-m_{\tilde{g}}m_t^2 B_0^q V_{5L}) \\
&\quad +m_t^2 V_1(m_{\tilde{g}}(B_0^g(m_t^2-u)(s+u)V_1+(m_t^2-t)t(B_0^m V_1-B_0^t V_2))V_{5R} \\
&\quad +m_t V_1V_{5L}(t(t-m_t^2)B_1^m)))) \qquad (37)
\end{aligned}$$

For vertex diagram Figs.1(f), (g) and (h), the non-zero form factors f_t^i are:

$$\begin{aligned}
f_v^1 &= \frac{1}{8\pi^2 st(t-m_t^2)}(V_{4L}(stV_1(C_0^l m_{\tilde{g}}m_t V_2V_{5L} \\
&\quad -(B_0^g V_2-2C_{00}^l V_2+2C_{00}^o V_1-(s+u)(C_{12}^l V_2-C_{12}^o V_1))V_{5R})
\end{aligned}$$

$$
\begin{aligned}
&+(m_t^2-t)(V_{5L}(t((-C_0m_{\tilde{g}}^2+C_0m_q^2+B_0^a-2C_{00}+C_1m_t^2)V_2\\
&-2C_{00}^dV_1)V_3+sV_1(V_2(B_0^g-2C_{00}^z+m_t^2C_1^z)-2V_1C_{00}^w))\\
&-m_{\tilde{g}}m_tV_2V_{5R}(C_0tV_3+sV_1C_0^z))))
\end{aligned}
\tag{38}
$$

$$
\begin{aligned}
f_v^3 &= \frac{1}{8\pi^2su(u-m_t^2)}(V_{4L}((m_t^2-u)(m_{\tilde{g}}m_tV_2V_{5R}(C_0uV_3-sV_1C_0^x)\\
&+V_{5L}(u(2C_{00}^dV_1-(-C_0m_{\tilde{g}}^2+C_0m_q^2+B_0^a-2C_{00}+C_1m_t^2)V_2)V_3\\
&+sV_1(V_2(B_0^m-2C_{00}^x+m_t^2C_2^x)-2V_1C_{00}^y)))-suV_1(m_{\tilde{g}}m_t(C_1^pV_2+C_1^rV_1)V_{5L}\\
&+((B_0^m-2C_{00}^p+C_{12}^pu)V_2+2C_{00}^rV_1-C_{12}^ruV_1)V_{5R})))
\end{aligned}
\tag{39}
$$

$$
\begin{aligned}
f_v^5 &= \frac{1}{8\pi^2}(V_1V_{4L}(\frac{2C_{00}^oV_1V_{5R}}{t-m_t^2}+\frac{V_2(C_0^lm_{\tilde{g}}m_tV_{5L}-B_0^gV_{5R}+2C_{00}^lV_{5R})}{m_t^2-t}\\
&+\frac{V_1(-m_{\tilde{g}}m_tV_{5L}C_1^r-2C_{00}^rV_{5R}+C_{12}^rV_{5R})}{m_t^2-u}\\
&-\frac{V_2(C_1^pm_{\tilde{g}}m_tV_{5L}+(B_0^m-2C_{00}^p+C_{00}^pu)V_{5R})}{m_t^2-t}\\
&-\frac{1}{t}(V_1(m_{\tilde{g}}m_tV_{5R}C_1^w+V_{5L}(2C_{00}^w-tC_{12}^w+m_t^2(C_1^w+C_{11}^w+C_{12}^w))))\\
&+\frac{V_2(V_{5L}(B_0^m-2C_{00}^x+m_t^2C_2^x)-m_{\tilde{g}}m_tV_{5R}C_0^x)}{u}-\frac{2V_1V_{5L}C_{00}^y}{u}\\
&+\frac{1}{t}(V_2(m_{\tilde{g}}m_tV_{5R}C_1^z+V_{5L}(B_0^g-2C_{00}^z+tC_{12}^z-m_t^2(C_{11}^z+C_{12}^z))))))
\end{aligned}
\tag{40}
$$

$$
\begin{aligned}
f_v^7 &= \frac{1}{8\pi^2su(u-m_t^2)}(V_{4L}(suV_1(m_{\tilde{g}}m_tC_0^pV_2V_{5L}\\
&-(B_0^mV_2-2C_{00}^p+2C_{00}^rV_1)V_{5R})+(m_t^2-u)(m_{\tilde{g}}m_tV_2V_{5R}(C_0uV_3-sV_1C_0^x)\\
&+V_{5L}(u(2C_{00}^dV_1-(-C_0m_{\tilde{g}}^2+C_0m_q^2+B_0^a-2C_{00}+C_1m_t^2)V_2)V_3\\
&+sV_1(V_2(B_0^m-2C_{00}^x+m_t^2C_2^x)-2V_1C_{00}^y)))))
\end{aligned}
\tag{41}
$$

$$
\begin{aligned}
f_v^9 &= \frac{1}{16\pi^2}(V_{4R}(\frac{1}{s(m_t^2-u)}(2sV_1(m_t(-B_0^mV_2+2C_{00}^pV_2\\
&-2C_{00}^rV_1)V_{5L}+m_{\tilde{g}}C_0^puV_2V_{5R})\\
&+(m_t^2-u)(m_{\tilde{g}}(C_0m_t^2V_2+C_2(t-u)V_2\\
&+(t-u)(C_1V_2-(C_0^d+C_1^d+C_2^d)V_1))V_{5L}\\
&+m_t(-B_0^aV_2+(2C_{00}+C_0(m_{\tilde{g}}-m_q)(m_{\tilde{g}}+m_q)+(C_{11}+C_{12})(t-u)\\
&-C_1(s+2u))V_2+2C_{00}^dV_1+(C_1^d+C_{11}^d+C_{12}^d)(t-u)V_1)V_{5R})V_3)\\
&+\frac{2V_1V_2(m_tuV_{5R}C_2^x-m_{\tilde{g}}uV_{5L}C_0^x)}{u}))
\end{aligned}
\tag{42}
$$

$$
\begin{aligned}
f_v^{11} &= \frac{1}{16\pi^2}(V_{4L}(\frac{1}{(m_t^2-u)(m_t^2-t)}(V_1(2(-(C_{00}^o+C_{00}^r)m_t^2 \\
&+C_{00}^r t+C_{00}^o u)V_1V_{5R}+V_2(m_{\tilde{g}}m_t(C_0^p(m_t^2-t)+C_0^l(m_t^2-u))V_{5L} \\
&+(-(B_0^m-2C_{00}^p)(m_t^2-t)+2C_{00}^l(m_t^2-u)+B_0^g(u-m_t^2))V_{5R}))) + \\
&\frac{1}{tu}(V_1(V_2(V_{5L}(t(V_0^m-2C_{00}^x+m_t^2C_2^x)+u(B_0^g-2C_{00}^z)+m_t^2uC_1^z) \\
&-m_{\tilde{g}}m_tV_{5R}(tC_0^x+uC_0^z))-2V_1V_{5L}(uC_{00}^w+tC_{00}^y))))) \qquad (43)\\
f_v^{13} &= \frac{1}{16\pi^2}(V_1V_{4R}(\frac{2m_tC_{00}^rV_1V_{5L}}{m_t^2-u}+m_{\tilde{g}}V_2C_0^xV_{5L}-\frac{C_0^lm_{\tilde{g}}(s+u)V_2V_{5R}}{m_t^2-t} \\
&+\frac{1}{m_t^2-u}(V_2(m_t(B_0^m-2C_{00}^p)V_{5L} \\
&-m_{\tilde{g}}C_0^puV_{5R}))+\frac{2m_tV_1V_{5R}C_{00}^w}{t}-m_tV_2V_{5R}C_2^x \\
&+\frac{1}{t}(V_2(m_{\tilde{g}}(s+u)V_{5L}C_0^z-m_tV_{5R}(B_0^g-2C_{00}^z+(s+u)C_1^z))))) \qquad (44)\\
f_v^{15} &= -\frac{1}{8\pi^2(m_t^2-t)}(V_1V_{4R}(C_{12}^lm_tV_2V_{5L}-m_tC_{12}^oV_1V_{5L} \\
&+m_{\tilde{g}}((C_0^l+C_2^l)V_2+C_2^oV_1)V_{5R})) \qquad (45)\\
f_v^{17} &= -\frac{1}{8\pi^2(m_t^2-t)}(V_{4L}((s+u)V_1(C_{12}^lV_2-C_{12}^oV_1)V_{5R} \qquad (46)\\
&+(m_t^2-t)V_1V_{5L}(V_2C_{12}^x+V_1C_{12}^y))) \qquad (47)\\
f_v^{19} &= \frac{1}{8\pi^2(m_t^2-t)u}(V_{4R}(uV_1(C_{12}^lm_tV_2V_{5L}-m_tC_{12}^oV_1V_{5L} \\
&+m_{\tilde{g}}((C_0^l+C_2^l)V_2+C_2^oV_1)V_{5R})+(m_t^2-t)V_1(m_{\tilde{g}}V_{5L}(V_1C_2^y-V_2(C_0^x+C_2^x)) \\
&+m_tV_{5R}(V_2(C_{12}^x+C_2^x+C_{22}^x)+V_1(C_{12}^y+C_2^y+C_{22}^y))))) \qquad (48)\\
f_v^{21} &= \frac{1}{8\pi^2(m_t^2-u)}(V_1V_{4R}(m_t(C_{12}^pV_2-C_{12}^rV_1)V_{5L} \\
&+m_{\tilde{g}}((C_0^p+C_1^p)V_2+C_1^rV_1)V_{5R})) \qquad (49)\\
f_v^{23} &= \frac{1}{8\pi^2t(m_t^2-u)}(V_{4R}((m_t^2-u)V_1(m_{\tilde{g}}V_{5L}(V_2(C_0^z+C_1^z)-V_1C_1^w) \\
&-m_tV_{5R}(V_1(C_1^w+C_{11}^w+C_{12}^w)+V_2(C_1^z+C_{11}^z+C_{12}^z)))-tV_1(m_t(C_{12}^pV_2 \\
&-C_{12}^rV_1)V_{5L}+m_{\tilde{g}}((C_0^p+C_1^p)V_2+C_1^rV_1)V_{5R}))) \qquad (50)\\
f_v^{25} &= \frac{1}{4\pi^2s(m_t^2-t)t}(V_{4R}(stV_1(C_{12}^lm_tV_2V_{5L}-m_tC_{12}^oV_1V_{5L} \\
&+m_{\tilde{g}}((C_0^l+C_2^l)V_2+C_2^oV_1)V_{5R})+(m_t^2-t)(t(m_{\tilde{g}}((C_1+C_2)V_2 \\
&-(C_0^d+C_1^d+C_2^d)V_1)V_{5L}+m_t((C_1+C_{11}+C_{12})V_2 \\
&+(C_1^d+C_{11}^d+C_{12}^d)V_1)V_{5R})V_3+sV_1(m_{\tilde{g}}V_{5L}(V_1C_1^w
\end{aligned}
$$

$$-V_2(C_0^z+C_1^z))+m_tV_{5R}(V_1(C_1^w+C_{11}^w+C_{12}^w)+V_2(C_1^z+C_{11}^z+C_{12}^z))))))\quad(51)$$

$$\begin{aligned}f_v^{27} &= \frac{1}{4\pi^2 su}(V_{4R}(sV_1(m_{\tilde{g}}V_{5L}(V_1C_2^y-V_2(C_0^x+C_2^x))\\ &+m_tV_{5R}(V_2(C_{12}^x+C_2^x+C_{22}^x)+V_1(C_{12}^y+C_2^y+C_{22}^y)))\\ &-u(m_{\tilde{g}}((C_1+C_2)V_2-(C_0^d+C_1^d+C_2^d)V_1)V_{5L}+m_t((C_1+C_{11}\\ &+C_{12})V_2+(C_1^d+C_{11}^d+C_{12}^d)V_1)V_{5R})V_3))\end{aligned}\quad(52)$$

$$\begin{aligned}f_v^{29} &= \frac{1}{4\pi^2(m_t^2-t)u}(V_{4R}((m_t^2-t)V_1(m_{\tilde{g}}V_{5L}(V_2(C_0^x+C_2^x)-V_1C_2^y)\\ &-m_tV_{5R}(V_2(C_{12}^x+C_2^x+C_{22}^x)+V_1(C_{12}^y+C_2^y+C_{22}^y)))-uV_1(C_{12}^l m_tV_2V_{5L}\\ &-m_tC_{12}^oV_1V_{5L}+m_{\tilde{g}}((C_0^l+C_2^l)V_2+C_2^oV_1)V_{5R})))\end{aligned}\quad(53)$$

And for box diagrams Figs.1(i)–(o), all form factors f_b^i are non-zero:

$$\begin{aligned}f_b^1 &= -\frac{1}{8\pi^2}(V_{4L}(C_2^f+C_0^g-2D_{00}^g+2D_{002}^g+2D_{003}^g-2D_{003}^s+(D_{13}^s+D_{23}^s)u\\ &+(D_{12}^g+D_{13}^g+D_{22}^g(s+u)+D_{23}^g(s+u)\\ &+D_2^gm_t^2)V_{5L}-D_0^gm_{\tilde{g}}m_tV_{5R})V_2^2\\ &+(2D_{003}^l+C_2^m-2D_{003}^n+D_{23}^nu)V_1V_{5L}V_2+2(D_{002}^f+D_{003}^f-D_{003}^m)V_1^2V_{5L}))\end{aligned}\quad(54)$$

$$\begin{aligned}f_b^3 &= -\frac{1}{8\pi^2}(V_{4L}(((C_0^f-C_0^g-C_1^g-C_2^g-2D_{001}^g-2D_{00}^s\\ &+2(D_{001}^s+D_{002}^s-(D_{13}^s+D_{23}^s)u)+(-D_{12}^s\\ &+D_{13}^s-D_{22}^s+D_{23}^s)u-D_{13}^g(s+u)\\ &+D_{12}^g(t-s))V_{5L}+m_{\tilde{g}}m_t(-D_1^g+D_1^s+D_2^s)V_{5R})V_2^2\\ &+V_1((-2D_{002}^l+D_2^l(m_q^2-m_{\tilde{g}}^2)+D_{12}^lm_t^2+C_1^n+2D_{002}^n+D_{22}^lu)V_{5L}\\ &-D_2^lm_{\tilde{g}}m_tV_{5R})V_2+2(-D_{001}^f+D_{001}^m+D_{002}^m)V_1^2V_{5L}))\end{aligned}\quad(55)$$

$$\begin{aligned}f_b^5 &= -\frac{1}{8\pi^2}(V_{4L}(((C_1^f+C_2^f+C_1^g+C_2^g+2D_{00}^g-2D_{002}^g+2D_{00}^s\\ &-2D_{002}^s+D_{23}^su+D_{22}^su\\ &+D_{23}^gt+D_{12}^gt)V_{5L}-m_{\tilde{g}}m_t(D_2^g\\ &+D_2^s)V_{5R})V_2^2+V_1((2D_{001}^l+2D_{002}^l+(D_1^l+D_2^l)(m_q^2-m_{\tilde{g}}^2)-(D_{11}^l+D_{12}^l)m_t^2\\ &+C_0^n+C_2^n-2(D_{001}^n+D_{002}^n)-(D_{12}^l+D_{22}^l)u)V_{5L}\\ &+(D_1^l+D_2^l)m_{\tilde{g}}m_tV_{5R})V_2-2(D_{002}^f+D_{002}^m)V_1^2V_{5L}))\end{aligned}\quad(56)$$

$$f_b^7 = \frac{1}{8\pi^2}(V_{4L}((m_{\tilde{g}}m_tD_0^sV_{5R}-(C_0^f+2D_{001}^g+2D_{002}^g+2D_{003}^g$$

$$
\begin{aligned}
& -2(2D^s_{00}+D^s_{001}+D^s_{002}+D^s_{003})+D^s_2 u)V_{5L})V_2^2 \\
& +2(-D^l_{002}-D^l_{003}+D^n_{00}+D^n_{002}+D^n_{003}V_1V_{5L}V_2 \\
& -2(D^f_{00}+D^f_{001}+D^f_{002}+D^f_{003}-D^m_{00}-D^m_{001}-D^m_{002}-D^m_{003})V_1^2V_{5L}))) \qquad (57)
\end{aligned}
$$

$$
\begin{aligned}
f_b^9 &= \frac{1}{16\pi^2}(V_{4R}(m_{\tilde{g}}V_{5L}(2(C^f_0-2(D^g_{00}+D^s_{00})-D^s_0 u)V_2^2 \\
& -4(D^l_{00}+D^n_{00})V_1V_2+4(D^f_{00}+D^m_{00})V_1^2+C^d_0V_7) \\
& +m_tV_{5R}(-2(-(D^s_2+D^s_3)m_t^2+C^f_1+C^f_2-2D^g_{001}2D^g_{002}+2D^s_{00} \\
& +D^s_{001}+m_t^2(D^s_2+2D^s_3)-D^s_2u-D^s_3m_t^2V_2^2-4(D^l_{00} \\
& -D^l_{001}-D^n_{001})V_1V_2+4(D^f_{00}+D^f_{001}+D^f_{002}-D^m_{001})V_3^2-C^d_1V_7)))) \qquad (58)
\end{aligned}
$$

$$
\begin{aligned}
f_b^{11} &= \frac{1}{16\pi^2}(V_2V_{4L}(V_2((C^f_0+C^g_0-4D^g_{00}-4D^s_{00}+D^s_2u+D^g_2t)V_{5L} \\
& -m_{\tilde{g}}m_t(D^g_0+D^s_0)V_{5R})-2(D^l_{00}+D^n_{00})V_3V_{5L})) \qquad (59)
\end{aligned}
$$

$$
\begin{aligned}
f_b^{13} &= \frac{1}{16\pi^2}(V_2V_{4R}(m_t((C^f_1+C^f_2+C^g_2+2D^g_{00}+2D^s_{00}-D^s_2u)V_2+2D^l_{00}V_1)V_{5R} \\
& -m_{\tilde{g}}(C^f_0-C^g_0-D^g_2s-D^g_0s-(D^g_0+D^s_0)u)V_2V_{5L})) \qquad (60)
\end{aligned}
$$

$$
\begin{aligned}
f_b^{15} &= \frac{1}{8\pi^2}(V_2V_{4R}(-m_{\tilde{g}}D^n_3V_1V_{5L}+m_tD^n_{13}V_1V_{5R}+V_2(m_{\tilde{g}}(D^g_0 \\
& +D^g_2+D^g_3-D^s_3)V_{5L}-m_t(D^g_{12}+D^g_{13}+D^g_2+D^g_{22}+D^g_{23}+D^s_{13})V_{5R}))) \qquad (61)
\end{aligned}
$$

$$
\begin{aligned}
f_b^{17} &= \frac{1}{8\pi^2}(((C^f_2+C^g_2+2D^g_{00}+2D^g_{002}+2(D^s_{00}+D^s_{002})+m_2^tD^s_{23}-D^s_{23}(s+t) \\
& -(D^s_{12}+D^s_2+D^s_{22}+D^s_{23})u+(D^g_{12}+D^g_2+D^g_{22}(s+u) \\
& -(2D^l_{001}+2D^l_{002}-C^m_2-2D^n_{00}-2D^n_{001}-2D^n_{002} \\
& +(D^n_{12}+D^n_2+D^n_{22})u)V_1V_2+2(D^f_{002}+D^m_{002})V_3^2)V_{4L}V_{5L}) \qquad (62)
\end{aligned}
$$

$$
\begin{aligned}
f_b^{19} &= \frac{1}{8\pi^2}(V_2V_{4R}(m_t((D^g_{12}+D^G_2+D^g_{22}-D^s_{12})V_2+(D^n_1+D^n_{11}+D^n_{12})V_1)V_{5R} \\
& -m_{\tilde{g}}((D^g_0+D^g_2+D^s_0+D^s_2)V_2+(D^n_0+D^n_1+D^n_2)V_1)V_{5L})) \qquad (63)
\end{aligned}
$$

$$
\begin{aligned}
f_b^{21} &= \frac{1}{8\pi^2}(V_2V_{4R}(m_{\tilde{g}}(D^g_1V_2-(D^s_0+D^s_1+D^s_2)V_2+D^l_2V_1)V_{5L}+m_t((D^g_{13}+ \\
& D^s_{12}+D^s_{13}+D^s_2+D^s_{22}+D^s_{23})V_2+(D^l_{12}+D^l_2+D^l_{22}+D^l_{23})V_1)V_{5R})) \qquad (64)
\end{aligned}
$$

$$
\begin{aligned}
f_b^{23} &= \frac{1}{8\pi^2}(V_2V_{4R}(m_{\tilde{g}}((D^g_0+D^g_2+D^s_0+D^s_2)V_2 \\
& -(D^n_1+D^l_2)V_1)V_{5L}-m_t((-D^g_{23}+D^s_2+D^s_{22}+D^s_{23})V_2 \\
& +(D^l_1+D^l_{11}+2D^l_{12}+D^l_{13}+D^l_2+D^l_{22}+D^l_{23})V_1)V_{5R})) \qquad (65)
\end{aligned}
$$

$$
f_b^{25} = -\frac{1}{4\pi^2}(V_{4R}(m_{\tilde{g}}((D^g_0-D^g_{22}-D^g_{23}+D^s_{23})V_2^2
$$

$$
\begin{aligned}
&+(D^l_{13}+D^l_{23}+D^n_{23}+D^n_{13})V_1V_2+(D^f_{22}+D^f_{23}-D^m_{23})V_1^2)V_{5L}\\
&+m_t((D^g_{122}+D^g_{123}+D^g_{22}+D^g_{222}+D^g_{223}+D^g_{23}-D^m_{23})V_2^2\\
&+(D^l_{133}+D^l_{123}-D^n_{133}-D^n_{123})V_1V_2\\
&+(D^f_{122}+D^f_{123}+D^f_{22}+D^f_{222}+D^f_{223}+D^f_{23}+D^m_{123})V_3^2)V_{5R}))
\end{aligned}
\tag{66}
$$

$$
\begin{aligned}
f_b^{27} &= \frac{1}{4\pi^2}(V_{4R}((m_{\tilde g}(-D^g_1-D^g_{12}+D^s_1+D^s_{12}+D^s_2+D^s_{22})V_{5L}\\
&+m_t(D^g_{112}+D^g_{122}+D^g_{12}+D^s_{112}+D^s_{122})V_{5R})V_2^2+V_1(m_{\tilde g}(D^l_{12}+D^l_{22}\\
&+D^n_{12}+D^n_2+D^n_{22})V_{5L}+m_t(D^l_{112}+D^l_{12}+D^l_{122}-D^n_{112}\\
&-D^n_{12}-D^n_{122})V_{5R})V_2+V_1^2((D^f_{12}-D^m_{12}-D^m_{22})m_{\tilde g}V_{5L}+(D^f_{112}+D^f_{12}\\
&+D^f_{122}+D^m_{112}+D^m_{122})m_tV_{5R})))
\end{aligned}
\tag{67}
$$

$$
\begin{aligned}
f_b^{29} &= -\frac{1}{4\pi^2}(V_{4R}((m_{\tilde g}(D^g_2+D^g_{22}+D^s_2+D^s_{22})V_{5L}\\
&-m_t(D^g_{122}+D^g_{22}+D^g_{222}-D^s_{122})V_{5R})V_2^2+V_1(m_{\tilde g}(D^l_{11}\\
&+2D^l_{12}+D^l_{22}+D^n_1+D^n_{11}+2D^n_{12}+D^n_2+D^n_{22})V_{5L}\\
&+m_t(D^l_{11}+D^l_{111}+2D^l_{112}+D^l_{12}+D^l_{122}-D^n_{11}-D^n_{111}-2D^n_{112}\\
&-D^n_{12}-D^n_{122})V_{5R})V_2-V_1^2((D^f_{22}+D^m_{22})m_{\tilde g}V_{5L}\\
&+(D^f_{122}+D^f_{22}+D^f_{222}+D^f_{122}-D^m_{122})m_tV_{5R})))
\end{aligned}
\tag{68}
$$

$$
\begin{aligned}
f_b^{31} &= \frac{1}{4\pi^2}(((D^g_{112}+D^g_{113}+D^g_{12}+D^g_{122}+2D^g_{123}+D^g_{13}+D^g_{133}\\
&-D^s_{113}-2D^s_{123}-D^s_{13}-D^s_{133}-D^s_{23}-D^s_{223}-D^s_{233})V_2^2\\
&+(D^l_{223}+D^l_{23}+D^l_{233}-D^n_{23}-D^n_{223}-D^n_{233})V_1V_2\\
&+(D^f_{112}+D^f_{113}+D^f_{12}+D^f_{122}+2D^f_{123}+D^f_{13}+D^f_{133}-D^m_{113}-2D^m_{123}\\
&-D^m_{13}-D^m_{133}-D^m_{223}-D^m_{23}-D^m_{233})V_1^2)V_{4L}V_{5L})
\end{aligned}
\tag{69}
$$

$$
\begin{aligned}
f_b^{33} &= \frac{1}{4\pi^2}(((D^g_{12}+D^g_{122}+D^g_{123}+D^g_{13}+D^g_2+2D^g_{22}+D^g_{222}+2D^g_{223}\\
&+2D^g_{23}+D^g_{233}+D^s_{123}+D^s_{13}+D^s_{223}+D^s_{23}+D^s_{233})V_2^2-(D^l_{123}+D^l_{13}\\
&+D^l_{133}+D^l_{223}+D^l_{23}+D^l_{233}-D^n_{123}-D^n_{223}-D^n_{133}\\
&-D^n_{23}-D^n_{233})V_1V_2+(D^f_{122}+D^f_{123}+D^f_{22}+D^f_{222}+2D^f_{223}+D^f_{23}\\
&+D^f_{233}+D^m_{123}+D^m_{223}+D^m_{23}+D^m_{233})V_1^2)V_{4L}V_{5L})
\end{aligned}
\tag{70}
$$

$$
f_b^{35} = \frac{1}{4\pi^2}(V_{4R}((m_{\tilde g}(D^g_{12}+D^g_{13}+D^s_{13}+D^s_{23})V_{5L}-m_t(D^g_{112}+D^g_{113}
$$

$$
\begin{aligned}
&+D^g_{12}+D^g_{122}+D^g_{123}+D^g_{13}-D^s_{113}-D^s_{123})V_{5R})V_2^2\\
&+V_1((m_{\tilde{g}}(D^l_{23}+D^n_{23})V_{5L}+m_t(D^l_{123}-D^n_{123})V_{5R}))V_2\\
&-V_1^2((D^f_{12}+D^f_{13}+D^m_{13}+D^m_{23})m_{\tilde{g}}V_{5L}+(D^f_{112}\\
&+D^f_{113}+D^f_{12}+D^f_{122}+D^f_{123}+D^f_{13}-D^m_{113}-D^m_{123})m_tV_{5R})))
\end{aligned}
\tag{71}
$$

$$
\begin{aligned}
f_b^{37} &= -\frac{1}{4\pi^2}(((D^g_{112}+D^g_{12}+D^g_{122}+D^g_{123}+D^g_{13}+D^s_{112}\\
&+2D^s_{12}+2D^s_{122}+D^s_{123}+D^s_{13}+D^s_2+2D^s_{22}+D^s_{222}\\
&+D^s_{223}+D^s_{23})V_2^2+(-D^l_{122}-D^l_{123}-D^l_{22}-D^l_{222}-D^l_{223}\\
&+D^n_{12}+D^n_{122}+D^n_{123}+D^n_2+2D^n_{22}+D^n_{222}+D^n_{223}\\
&+D^n_{23})V_1V_2+(D^f_{112}+D^f_{123}+D^f_{12}+D^f_{122}+D^m_{112}+D^m_{12}\\
&+2D^m_{122}+D^m_{123}+D^m_{22}+D^m_{222}+D^m_{223})V_1^2)V_{4L}V_{5L})
\end{aligned}
\tag{72}
$$

$$
\begin{aligned}
f_b^{39} &= \frac{1}{4\pi^2}(((-D^g_{12}-D^g_{122}-D^g_2-2D^g_{22}-D^g_{222}-D^g_{223}\\
&-D^g_{23}+D^s_{12}+D^s_{122}+D^s_2+2D^s_{22}+D^s_{222}+D^s_{223}\\
&+D^s_{23})V_2^2+(-D^l_{112}-D^l_{113}-D^l_{12}-2D^l_{122}-2D^l_{123}-D^l_{22}-D^l_{222}-D^l_{223}\\
&+D^n_{112}+D^n_{113}+2D^n_{12}+2D^n_{122}+2D^n_{123}+D^n_{13}+D^n_2+2D^n_{22}\\
&+D^n_{222}+D^n_{223}+D^n_{23})V_1V_2+(-D^f_{122}-D^f_{22}-D^f_{222}-D^f_{223}\\
&+D^m_{122}+D^m_{22}+D^m_{222}+D^m_{223})V_1^2)V_{4L}V_{5L})
\end{aligned}
\tag{73}
$$

For the quarks initiated subprocesses, we list all form factors of $c\bar{c}$ initial state:

$$g^{6LR}_{s_4} = g^{14LR}_{s_4} = \frac{m_{\tilde{g}}B_0^tV_1^2V_{4R}V_{5R}}{8m_t\pi^2t} \tag{74}$$

$$g^{6RL}_{s_4} = g^{14LL}_{s_4} = g^{6LR}_{s_4}(V_{4L}\leftrightarrow V_{4R}, V_{5L}\leftrightarrow V_{5R}) \tag{75}$$

$$g^{6LR}_{s_3} = g^{14LR}_{s_3} = \frac{V_1^2V_{4R}(B_1m_t^2V_{5R}-m_{\tilde{g}}m_tB_0^qV_{5L})}{8m_t^2\pi^2t} \tag{76}$$

$$g^{6RL}_{s_3} = g^{14LL}_{s_3} = g^{6LR}_{s_3}(V_{4L}\leftrightarrow V_{4R}, V_{5L}\leftrightarrow V_{5R}) \tag{77}$$

$$g^{5LR}_{s_2} = g^{14RR}_{s_2} = \frac{V_1^2V_{4R}(m_{\tilde{g}}m_tB_0^qV_{5L}-B_1^qm_t^2V_{5R}}{8m_t^2\pi^2s} \tag{78}$$

$$g^{5RL}_{s_2} = g^{14RL}_{s_2} = g^{5LR}_{s_2}(V_{4L}\leftrightarrow V_{4R}, V_{5L}\leftrightarrow V_{5R}) \tag{79}$$

$$g^{5LR}_{s_1} = g^{14RR}_{s_1} = -\frac{m_{\tilde{g}}B_0^tV_1^2V_{4R}V_{5R}}{8m_t\pi^2s} \tag{80}$$

$$g^{5RL}_{s_1} = g^{14RL}_{s_1} = g^{5LR}_{s_1}(V_{4L}\leftrightarrow V_{4R}, V_{5L}\leftrightarrow V_{5R}) \tag{81}$$

$$g^{2LL}_{v_4} = g^{2LR}_{v_4} = \frac{1}{8\pi^2t}(V_1V_1V_{4R}(m_t(C_1^q+C_{11}^q$$

$$+C_{12}^q)V_{5R} - m_{\tilde{g}}(C_0^q + C_1^q + C_2^q)V_{5L})) \tag{82}$$

$$g_{v_4}^{2RL} = g_{v_4}^{2RR} = g_{v_4}^{2LL}(V_{4L} \leftrightarrow V_{4R}, V_{5L} \leftrightarrow V_{5R}) \tag{83}$$

$$g_{v_4}^{6LR} = g_{v_4}^{14LR} = \frac{C_{00}^q V_1 V_1 V_{4R} V_{5R}}{4\pi^2 t} \tag{84}$$

$$g_{v_4}^{6RL} = g_{v_4}^{14LL} = g_{v_4}^{6LR}(V_{4L} \leftrightarrow V_{4R}, V_{5L} \leftrightarrow V_{5R}) \tag{85}$$

$$g_{v_3}^{2LL} = g_{v_3}^{2LR} = -\frac{1}{8\pi^2 t}(V_1 V_2 V_{4R}(m_{\tilde{g}}(C_1^t + C_2^t)V_{5L} + m_t(C_1^t + C_{11}^t + C_{12}^t)V_{5R})) \tag{86}$$

$$g_{v_3}^{2RL} = g_{v_3}^{2RR} = g_{v_3}^{2LL}(V_{4L} \leftrightarrow V_{4R}, V_{5L} \leftrightarrow V_{5R}) \tag{87}$$

$$g_{v_3}^{6LR} = g_{v_3}^{14LR} = -\frac{1}{8\pi^2 t}(V_1 V_2 V_{4R}(C_0^t V_{5R} m_{\tilde{g}}^2 + m_t C_0^t V_{5L} m_{\tilde{g}}$$
$$-(C_0^t m_q^2 + B_0^d - 2C_{00}^t + m_t^2 C_1^t)V_{5R})) \tag{88}$$

$$g_{v_3}^{6RL} = g_{v_3}^{14LL} = g_{v_3}^{6LR}(V_{4L} \leftrightarrow V_{4R}, V_{5L} \leftrightarrow V_{5R}) \tag{89}$$

$$g_{v_2}^{5LR} = g_{v_2}^{14RR} = \frac{C_{00}^d V_1 V_1 V_{4R} V_{5R}}{4\pi^2 s} \tag{90}$$

$$g_{v_2}^{5RL} = g_{v_2}^{14RL} = g_{v_2}^{5LR}(V_{4L} \leftrightarrow V_{4R}, V_{5L} \leftrightarrow V_{5R}) \tag{91}$$

$$g_{v_2}^{8LL} = g_{v_2}^{8LR} = \frac{1}{8\pi^2 s}(V_1 V_1 V_{4R}((C_1^d + C_{11}^d + C_{12}^d)m_t V_{5R}$$
$$-(C_0^d + C_1^d + C_2^d)m_{\tilde{g}} V_{5L})) \tag{92}$$

$$g_{v_2}^{8RL} = g_{v_2}^{8RR} = g_{v_2}^{8LL}(V_{4L} \leftrightarrow V_{4R}, V_{5L} \leftrightarrow V_{5R}) \tag{93}$$

$$g_{v_1}^{5LR} = g_{v_1}^{14RR} = \frac{1}{8\pi^2 s}(V_1 V_2 V_{4R}(C_0 m_{\tilde{g}} m_t V_{5L}$$
$$-(-C_0 m_{\tilde{g}}^2 + C_0 m_q^2 + B_0^a - 2C_{00} + C_1 m_2^t)V_{5R})) \tag{94}$$

$$g_{v_1}^{5RL} = g_{v_1}^{14RL} = g_{v_1}^{5LR}(V_{4L} \leftrightarrow V_{4R}, V_{5L} \leftrightarrow V_{5R}) \tag{95}$$

$$g_{v_1}^{8LL} = g_{v_1}^{8LR} = \frac{V_1 V_2 V_{4R}((C_1 + C_2)m_{\tilde{g}} V_{5L} + (C_1 + C_{11} + C_{12})m_t V_{5R})}{8\pi^2 s} \tag{96}$$

$$g_{v_1}^{8RL} = g_{v_1}^{8RR} = g_{v_1}^{8LL}(V_{4L} \leftrightarrow V_{4R}, V_{5L} \leftrightarrow V_{5R}) \tag{97}$$

$$g_{b_4}^{1LL} = \frac{m_{\tilde{g}} D_3^q V_{4R}^3 V_{5L}}{16\pi^2} \tag{98}$$

$$g_{b_4}^{1RR} = g_{b_4}^{1LL}(V_{4L} \leftrightarrow V_{4R}, V_{5L} \leftrightarrow V_{5R}) \tag{99}$$

$$g_{b_4}^{1LR} = \frac{m_{\tilde{g}} D_3^q V_{4R}^2 V_{4L} V_{5R}}{16\pi^2} \tag{100}$$

$$g_{b_4}^{1RL} = g_{b_4}^{1LR}(V_{4L} \leftrightarrow V_{4R}, V_{5L} \leftrightarrow V_{5R}) \tag{101}$$

$$g_{b_4}^{4LL} = \frac{m_{\tilde{g}} V_{4L} V_{4R}^2 (m_{\tilde{g}} D_0^q V_{5L} + m_t (D_0^q + D_1^q + D_2^q)V_{5R})}{16\pi^2} \tag{102}$$

$$g_{b_4}^{4RR} = g_{b_4}^{4LL}(V_{4L} \leftrightarrow V_{4R}, V_{5L} \leftrightarrow V_{5R}) \tag{103}$$

$$g_{b_4}^{4LR} = \frac{m_{\tilde{g}} V_{4L}^3 (m_{\tilde{g}} D_0^q V_{5L} + m_t (D_0^q + D_1^q + D_2^q)V_{5R})}{16\pi^2} \tag{104}$$

$$g_{b_4}^{4RL} = g_{b_4}^{4LR}(V_{4L} \leftrightarrow V_{4R}, V_{5L} \leftrightarrow V_{5R}) \quad (105)$$

$$g_{b_4}^{9LL} = g_{b_4}^{9LR} = \frac{D_{13}^q V_{4L} V_{4R}^2 V_{5L}}{16\pi^2} \quad (106)$$

$$g_{b_4}^{9RL} = g_{b_4}^{9RR} = g_{b_4}^{9LL}(V_{4L} \leftrightarrow V_{4R}, V_{5L} \leftrightarrow V_{5R}) \quad (107)$$

$$g_{b_4}^{11LL} = g_{b_4}^{11LR} = \frac{V_{4L}^2 V_{4R}(m_{\tilde{g}} D_1^q V_{5L} + m_t(D_1^q + D_{11}^q + D_{12}^q)V_{5R})}{16\pi^2} \quad (108)$$

$$g_{b_4}^{11RL} = g_{b_4}^{11RR} = g_{b_4}^{11LL}(V_{4L} \leftrightarrow V_{4R}, V_{5L} \leftrightarrow V_{5R}) \quad (109)$$

$$g_{b_4}^{13LL} = g_{b_4}^{13RL} = \frac{D_{00}^q V_{4L} V_{4R}^2 V_{5L}}{8\pi^2} \quad (110)$$

$$g_{b_4}^{13LR} = g_{b_4}^{13RR} = g_{b_4}^{13LL}(V_{4L} \leftrightarrow V_{4R}, V_{5L} \leftrightarrow V_{5R}) \quad (111)$$

$$g_{b_3}^{1LL} = -\frac{m_{\tilde{g}} D_3^t V_{4R}^3 V_{5L}}{16\pi^2} \quad (112)$$

$$g_{b_3}^{1RR} = g_{b_3}^{1LL}(V_{4L} \leftrightarrow V_{4R}, V_{5L} \leftrightarrow V_{5R}) \quad (113)$$

$$g_{b_3}^{1LR} = -\frac{m_{\tilde{g}} D_3^t V_{4R}^2 V_{4L} V_{5R}}{16\pi^2} \quad (114)$$

$$g_{b_3}^{1RL} = g_{b_3}^{1LR}(V_{4L} \leftrightarrow V_{4R}, V_{5L} \leftrightarrow V_{5R}) \quad (115)$$

$$g_{b_3}^{4LL} = \frac{m_{\tilde{g}} V_{4L} V_{4R}^2 (m_{\tilde{g}} D_0^t V_{5L} - m_t D_2^t V_{5R})}{16\pi^2} \quad (116)$$

$$g_{b_3}^{4RR} = g_{b_3}^{4LL}(V_{4L} \leftrightarrow V_{4R}, V_{5L} \leftrightarrow V_{5R}) \quad (117)$$

$$g_{b_3}^{4LR} = \frac{m_{\tilde{g}} V_{4L}^3 (m_{\tilde{g}} D_0^t V_{5L} - m_t D_2^t V_{5R})}{16\pi^2} \quad (118)$$

$$g_{b_3}^{4RL} = g_{b_3}^{4LR}(V_{4L} \leftrightarrow V_{4R}, V_{5L} \leftrightarrow V_{5R}) \quad (119)$$

$$g_{b_3}^{9LL} = g_{b_3}^{9LR} = \frac{D_{13}^t V_{4L} V_{4R}^2 V_{5L}}{16\pi^2} \quad (120)$$

$$g_{b_3}^{9RL} = g_{b_3}^{9RR} = g_{b_3}^{9LL}(V_{4L} \leftrightarrow V_{4R}, V_{5L} \leftrightarrow V_{5R}) \quad (121)$$

$$g_{b_3}^{11LL} = g_{b_3}^{11LR} = \frac{V_{4L}^2 V_{4R}(m_t D_{12}^t V_{5R} - m_{\tilde{g}} D_1^t V_{5L})}{16\pi^2} \quad (122)$$

$$g_{b_3}^{11RL} = g_{b_3}^{11RR} = g_{b_3}^{11LL}(V_{4L} \leftrightarrow V_{4R}, V_{5L} \leftrightarrow V_{5R}) \quad (123)$$

$$g_{b_3}^{13LL} = g_{b_3}^{13RL} = -\frac{D_{00}^t V_{4L} V_{4R}^2 V_{5L}}{8\pi^2} \quad (124)$$

$$g_{b_3}^{13LR} = g_{b_3}^{13RR} = g_{b_3}^{13LL}(V_{4L} \leftrightarrow V_{4R}, V_{5L} \leftrightarrow V_{5R}) \quad (125)$$

$$g_{b_2}^{2LL} = \frac{V_{4L}^2 V_{4R}(m_{\tilde{g}} V_{5L} D_3^v - m_t V_{5R} D_{23}^v)}{16\pi^2} \quad (126)$$

$$g_{b_2}^{2RR} = g_{b_2}^{2LL}(V_{4L} \leftrightarrow V_{4R}, V_{5L} \leftrightarrow V_{5R}) \quad (127)$$

$$g_{b_2}^{2LR} = \frac{V_{4R}^3 (m_{\tilde{g}} V_{5L} D_3^v - m_t V_{5R} D_{23}^v)}{16\pi^2} \quad (128)$$

$$g_{b_2}^{2RL} = g_{b_2}^{2LR}(V_{4L} \leftrightarrow V_{4R}, V_{5L} \leftrightarrow V_{5R}) \quad (129)$$

$$g_{b_2}^{5RR} = g_{b_2}^{5RL} = \frac{m_{\tilde{g}} V_{4L}^2 V_{4R}(m_{\tilde{g}} V_{5R} D_0^v - m_t V_{5L} D_2^v)}{16\pi^2} \quad (130)$$

$$g_{b_2}^{5LL} = g_{b_2}^{5LR} = g_{b_2}^{5RR}(V_{4L} \leftrightarrow V_{4R}, V_{5L} \leftrightarrow V_{5R}) \quad (131)$$

$$g_{b_2}^{6LR} = \frac{V_{4L}^2 V_{4R} V_{5R} D_{00}^v}{8\pi^2} \quad (132)$$

$$g_{b_2}^{6RL} = g_{b_2}^{6LR}(V_{4L} \leftrightarrow V_{4R}, V_{5L} \leftrightarrow V_{5R}) \quad (133)$$

$$g_{b_2}^{10LL} = -\frac{V_{4L}^3 V_{5L} D_{13}^v}{16\pi^2} \quad (134)$$

$$g_{b_2}^{10RR} = g_{b_2}^{10LL}(V_{4L} \leftrightarrow V_{4R}, V_{5L} \leftrightarrow V_{5R}) \quad (135)$$

$$g_{b_2}^{10LR} = -\frac{V_{4L}^2 V_{4R} V_{5L} D_{13}^v}{16\pi^2} \quad (136)$$

$$g_{b_2}^{10RL} = g_{b_2}^{10LR}(V_{4L} \leftrightarrow V_{4R}, V_{5L} \leftrightarrow V_{5R}) \quad (137)$$

$$g_{b_2}^{12LL} = g_{b_2}^{12LR} = -\frac{m_{\tilde{g}} V_{4L}^2 V_{4R} V_{5L} D_1^v}{16\pi^2} \quad (138)$$

$$g_{b_2}^{12RL} = g_{b_2}^{12RR} = g_{b_2}^{12LL}(V_{4L} \leftrightarrow V_{4R}, V_{5L} \leftrightarrow V_{5R}) \quad (139)$$

$$g_{b_2}^{14LL} = \frac{V_{4L}^3 V_{5L} D_{00}^v}{8\pi^2} \quad (140)$$

$$g_{b_2}^{14LR} = g_{b_2}^{14LL}(V_{4L} \leftrightarrow V_{4R}, V_{5L} \leftrightarrow V_{5R}) \quad (141)$$

$$g_{b_1}^{3LL} = g_{b_1}^{3RL} = \frac{(D_0 + D_1 + D_2 + D_3) m_{\tilde{g}} V_{4L}^2 V_{4R} V_{5L}}{16\pi^2} \quad (142)$$

$$g_{b_1}^{3LR} = g_{b_1}^{3RR} = g_{b_1}^{3LL}(V_{4L} \leftrightarrow V_{4R}, V_{5L} \leftrightarrow V_{5R}) \quad (143)$$

$$g_{b_1}^{5LR} = -\frac{D_{00} V_{4L}^2 V_{4R} V_{5R}}{8\pi^2} \quad (144)$$

$$g_{b_1}^{5RL} = g_{b_1}^{5LR}(V_{4L} \leftrightarrow V_{4R}, V_{5L} \leftrightarrow V_{5R}) \quad (145)$$

$$g_{b_1}^{6LL} = g_{b_1}^{6RL} = -\frac{m_{\tilde{g}} V_{4L} V_{4R}^2 (D_0 m_{\tilde{g}} V_{5L} + (D_0 + D_1 + D_2) m_t V_{5R})}{16\pi^2} \quad (146)$$

$$g_{b_1}^{6LR} = g_{b_1}^{6RR} = g_{b_1}^{6LL}(V_{4L} \leftrightarrow V_{4R}, V_{5L} \leftrightarrow V_{5R}) \quad (147)$$

$$g_{b_1}^{7LL} = \frac{(D_{12} + D_2 + D_{22} + D_{23}) V_{4L}^3 V_{5L}}{16\pi^2} \quad (148)$$

$$g_{b_1}^{7RR} = g_{b_1}^{7LL}(V_{4L} \leftrightarrow V_{4R}, V_{5L} \leftrightarrow V_{5R}) \quad (149)$$

$$g_{b_1}^{7LR} = \frac{(D_{12} + D_2 + D_{22} + D_{23}) V_{4L}^2 V_{4R} V_{5R}}{16\pi^2} \quad (150)$$

$$g_{b_1}^{7RL} = g_{b_1}^{7LR}(V_{4L} \leftrightarrow V_{4R}, V_{5L} \leftrightarrow V_{5R}) \quad (151)$$

$$g_{b_1}^{8LL} = -\frac{V_{4L}^2 V_{4R} (D_2 m_{\tilde{g}} V_{5L} + (D_{12} + D_2 + D_{22}) m_t V_{5R})}{16\pi^2} \quad (152)$$

$$g_{b_1}^{8RR} = g_{b_1}^{8LL}(V_{4L} \leftrightarrow V_{4R}, V_{5L} \leftrightarrow V_{5R}) \quad (153)$$

$$g_{b_1}^{8LR} = -\frac{V_{4R}^3 (D_2 m_{\tilde{g}} V_{5L} + (D_{12} + D_2 + D_{22}) m_t V_{5R})}{16\pi^2} \quad (154)$$

$$g_{b_1}^{8RL} = g_{b_1}^{8LR}(V_{4L} \leftrightarrow V_{4R}, V_{5L} \leftrightarrow V_{5R}) \quad (155)$$

$$g_{b_1}^{14RL} = -\frac{D_{00} V_{4L}^3 V_{5L}}{8\pi^2} \quad (156)$$

$$g_{b_1}^{14RR} = g_{b_1}^{14RL}(V_{4L} \leftrightarrow V_{4R}, V_{5L} \leftrightarrow V_{5R}) \quad (157)$$

$$(158)$$

References

[1] S. L. Glashow, J. Iliopoulos and L. Maiani, *Phys. Rev.* **D2** (1970) 1285.

[2] K. Hagiwara, *et al. Phys. Rev.* **D66** (2002) 010001.

[3] A.H. Chamseddine, R. Arnowitt and P. Nath, Phys. Rev. Lett. **49** (1982) 970; R. Barbieri, S. Ferrara and C.A. Savoy, Phys. Lett. **B119** (1982) 343; L. Hall, J. Lykken and S. Weinberg, Phys. Rev. **D27** (1983) 2359.

[4] N. Arkani-Hamed, J. March-Russell and H. Murayama, Nucl. Phys. **B509** (1998) 3; H. Murayama, Phys. Rev. Lett. **79** (1997) 18; K.-I. Izawa, Y. Nomura, K. Tobe and T. Yanagida, Phys. Rev. **D56** (1997) 2886; M.A. Luty, Phys. Lett. **B414** (1997) 71.

[5] L. Randall and R. Sundrum, Nucl. Phys. **B557** (1999) 79; G.F. Giudice, M.A. Luty, H. Murayama and R. Rattazzi, JHEP 9812 (1998) 027; J. Bagger, T. Moroi and E. Poppitz, JHEP 0004 (2000) 009; T. Gherghetta, G.F. Giudice and J.D. Wells, Nucl. Phys. **B559** (1999) 27.

[6] See e.g., D.E. Kaplan and G.D. Kribs, JHEP 0009 (2000) 048.

[7] T. Kobayashi and K. Yoshioka, Phys. Rev. Lett. **85** (2000) 5527.

[8] See, S. Bejar, J. Guasch and J. Sola, KA-TP-1-2001, UAB-FT-506, hep-ph/0101294 and references there in.

[9] C.S. Li, R.J. Oakes and J.M. Yang, *Phys. Rev.* **D49** (1994) 293; *Phys. Rev.* **D56** (1997) 3156, Erratum; G. Couture, C. Hamzaoui and H. König, *Phys. Rev.* **D52** (1995) 1713; G. Couture, M. Frank and H. König, *Phys. Rev.* **D56** (1997) 4213; J.L. Lopez, D.V. Nanopoulos and R. Rangarajan, *Phys. Rev.* **D56** (1997) 3100; G.M. de Divitiis, R. Petronzio and L. Silvestrini, *Nucl. Phys.* **B504** (1997) 45.

[10] J.J. Liu, C.S. Li, L.L. Yang and L.G. Jin, Phys. Lett. **B599** (2004) 92.

[11] J.M. Yang and C.S. Li, *Phys. Rev.* **D49** (1994) 3412; *Phys. Rev.* **D51** (1995) 3974, Erratum; J. Guasch and J. Sola, *Nucl. Phys.* **B562** (1999) 3.

[12] E. Malkawi and T. Tait, *Phys. Rev.* **D54** (1996) 5758.

[13] M. Hosch, K. Whisnant and B.-L. Young, *Phys. Rev.* **D56** (1997) 5725.

[14] T. Han, M. Hosch, K. Whisnant, B.-L. Young and X. Zhang, *Phys. Rev.* **D58** (1998) 073008.

[15] A. Belyaev and N. Kidonakis, *Phys. Rev.* **D65** (2002) 037501.

[16] Y.P. Gouz and S.R. Slabospitsky, *Phys. Lett.* **B457** (1999) 177.

[17] C.S. Li, X. Zhang and S.H. Zhu, *Phys. Rev.* **D60** (1999) 077702; Zhou Hong, Ma Wen-Gan, Jiang Yi, Zhang Ren-You and Wan Lang-Hui, *Phys. Rev.* **D64** (2001) 095006; Zhou Hong, Ma Wen-Gan and Zhang Ren-You, hep-ph/0208170; C. Yue, Y. Dai, Q. Xu and G. Liu, *Phys. Lett.* **B525** (2002) 301; J. Cao, Z. Xiong and J.M. Yang, *Nucl. Phys.* **B651** (2003) 87; *Phys. Rev.* **D67** (2003) 071701.

[18] L.J. Hall, V.A. Kostelecky and S. Raby, *Nucl. Phys.* **B267** (1986) 415.

[19] T. Besmer, C. Greub and T. Hurth, *Nucl. Phys.* **B609** (2001) 359.

[20] R. Harnik, D.T. Larson, H. Murayama and A. Pierce, *Phys. Rev.* **D69** (2004) 094024; D.A. Demir, Phys. Lett. **B571** (2003) 193; A.M. Curiel, M.J. Herrero, and D. Temes, *Phys. Rev.* **D67** (2003) 075008.

[21] M. Misiak, S. Pokorski and J. Rosiek, in "Heavy Flavours 2", eds. A.J. Buras and M. Lindner, Advanced Series on Directions in High Energy Physics, World Scientific Publishing Co., Singapore, hep-ph/9703442.

[22] F. Gabbiani, E. Gabrielli, A. Masiero and L. Silvestrini, *Nucl. Phys.* **B477** (1996) 321.

[23] J. Pumplin, D.R. Stump, J. Huston, H.L. Lai, P. Nadolsky and W.K. Tung, JHEP 0207 (2002) 012.

[24] E. Gabrielli and S. Khalil *Phys. Rev.* **D67** (2003) 015008.

[25] J.P. Saha and A. Kundu, *Phys. Rev.* **D69** (2004) 016004.

[26] S. Khalil and O. Lebedev, *Phys. Lett.* **B515** (2001) 387.

[27] S. Prelovsek and D. Wyler, *Phys. Lett.* **B500** (2001) 304.

[28] M.B. Causse and J. Orloff, *Eur. Phys. J.* **C23** (2002) 749.

[29] G. Passarino and M. Veltman, Nucl. Phys. **B160**, 151 (1979); A. Denner, Fortschr. Phys. **41**, 4 (1993).

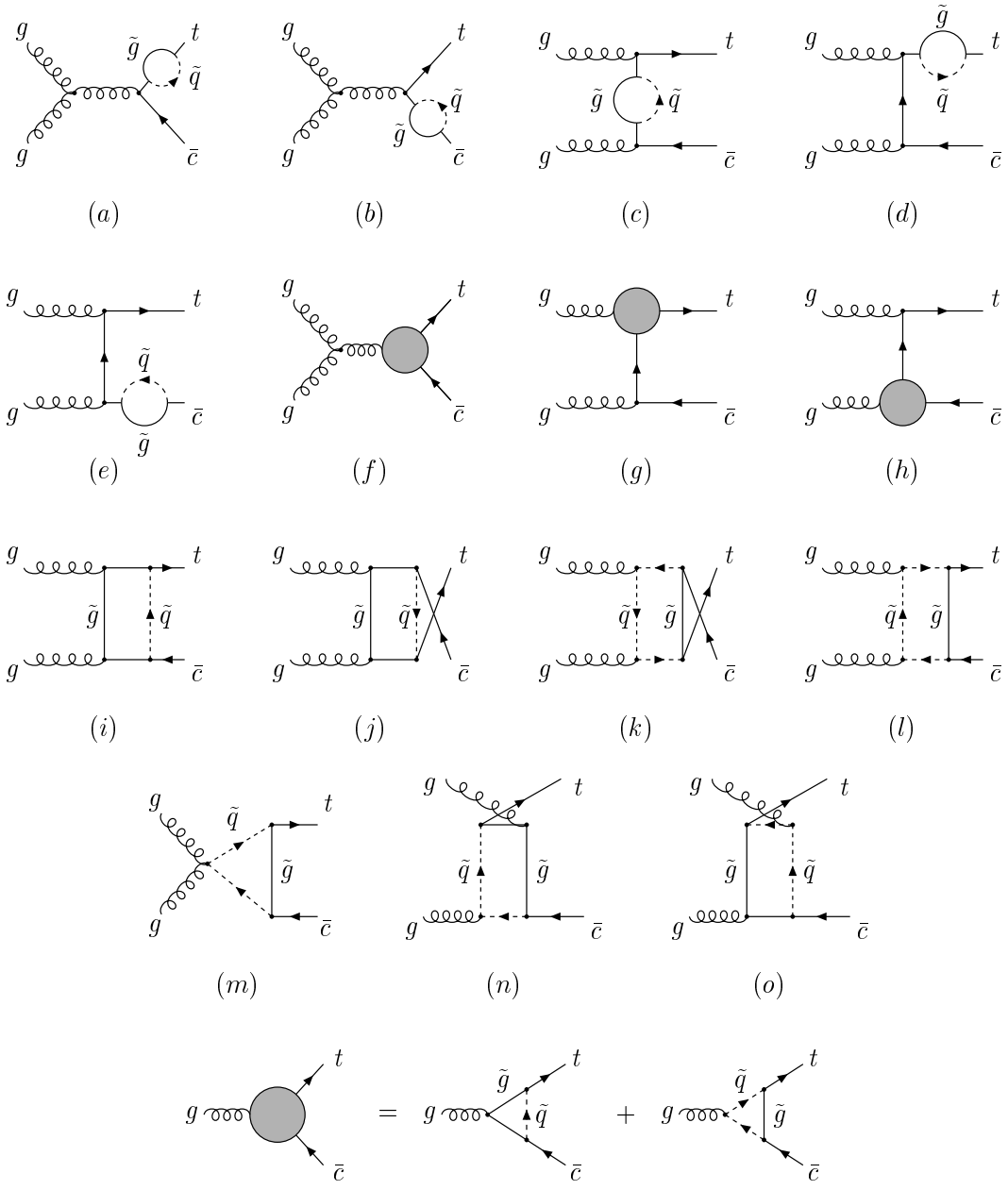

Figure 1: Gluon initial state subprocess Feynman diagrams for the top quark and anti-charm quark associated production.

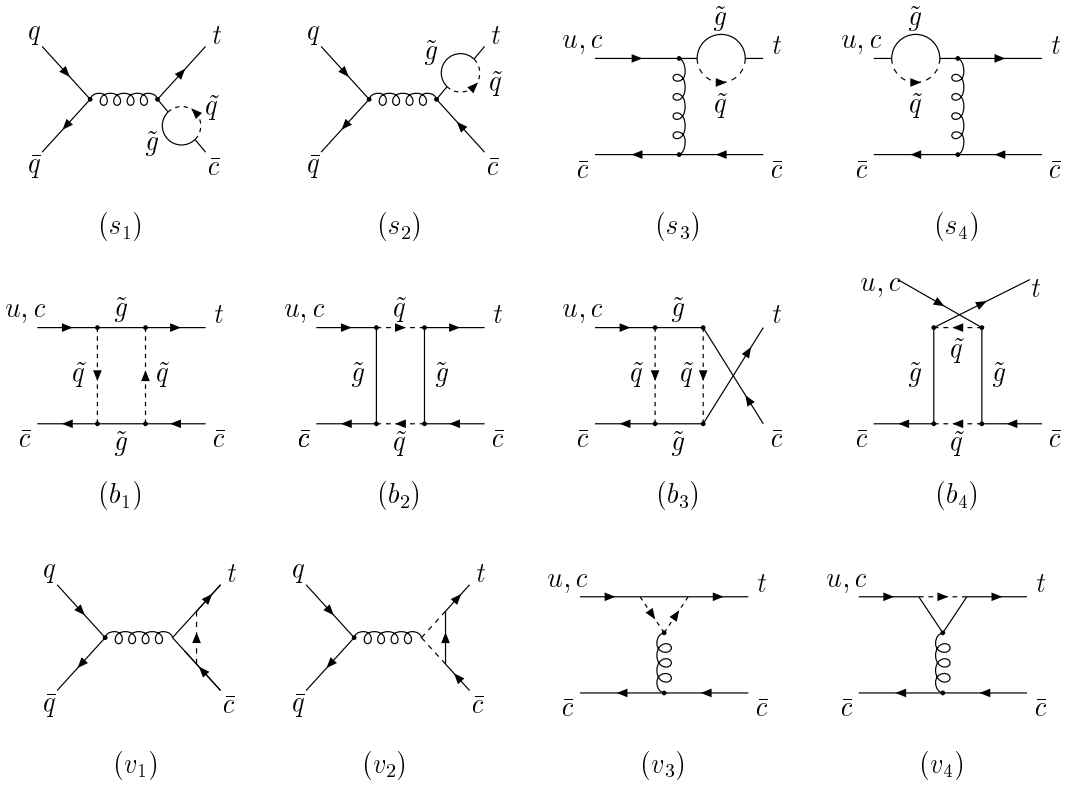

Figure 2: Quark initial state subprocess Feynman diagrams for the top quark and anti-charm quark associated production.

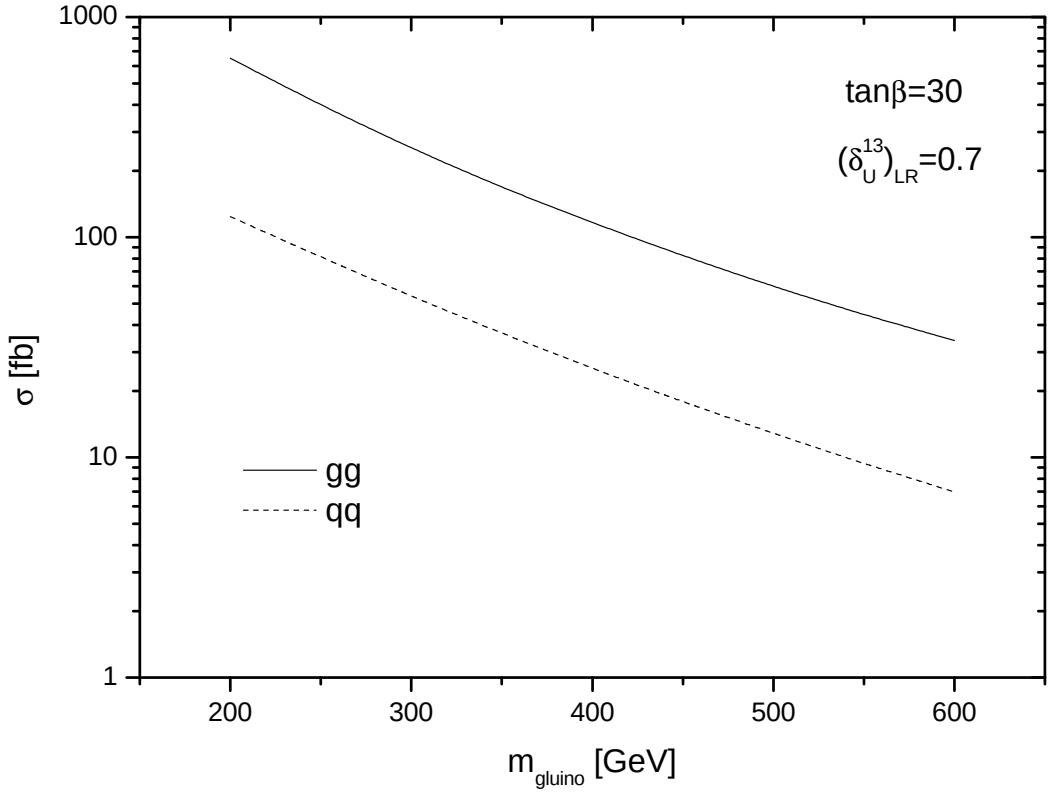

Figure 3: The total cross sections for the $pp \to t\bar{u}$ as a function of the mass of gluino.

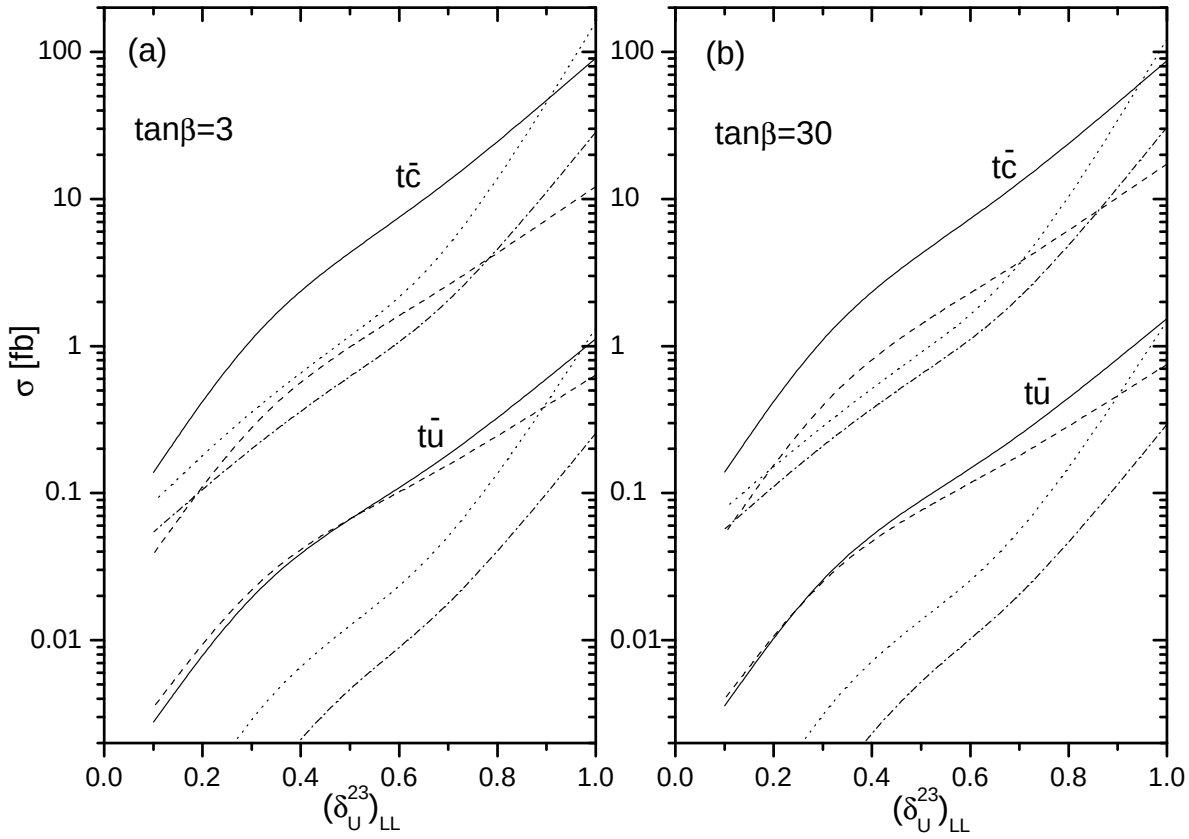

Figure 4: The total cross sections for the $pp \to t\bar{c}(\bar{u})$ with LL off-diagonal elements. Here, solid line: $m_{\tilde{g}} = 200$ GeV, $M_{\rm SUSY} = 400$ GeV; dashed line: $m_{\tilde{g}} = 300$ GeV, $M_{\rm SUSY} = 400$ GeV; dotted line: $m_{\tilde{g}} = 200$ GeV, $M_{\rm SUSY} = 1000$ GeV; dash-dotted line: $m_{\tilde{g}} = 300$ GeV, $M_{\rm SUSY} = 1000$ GeV.

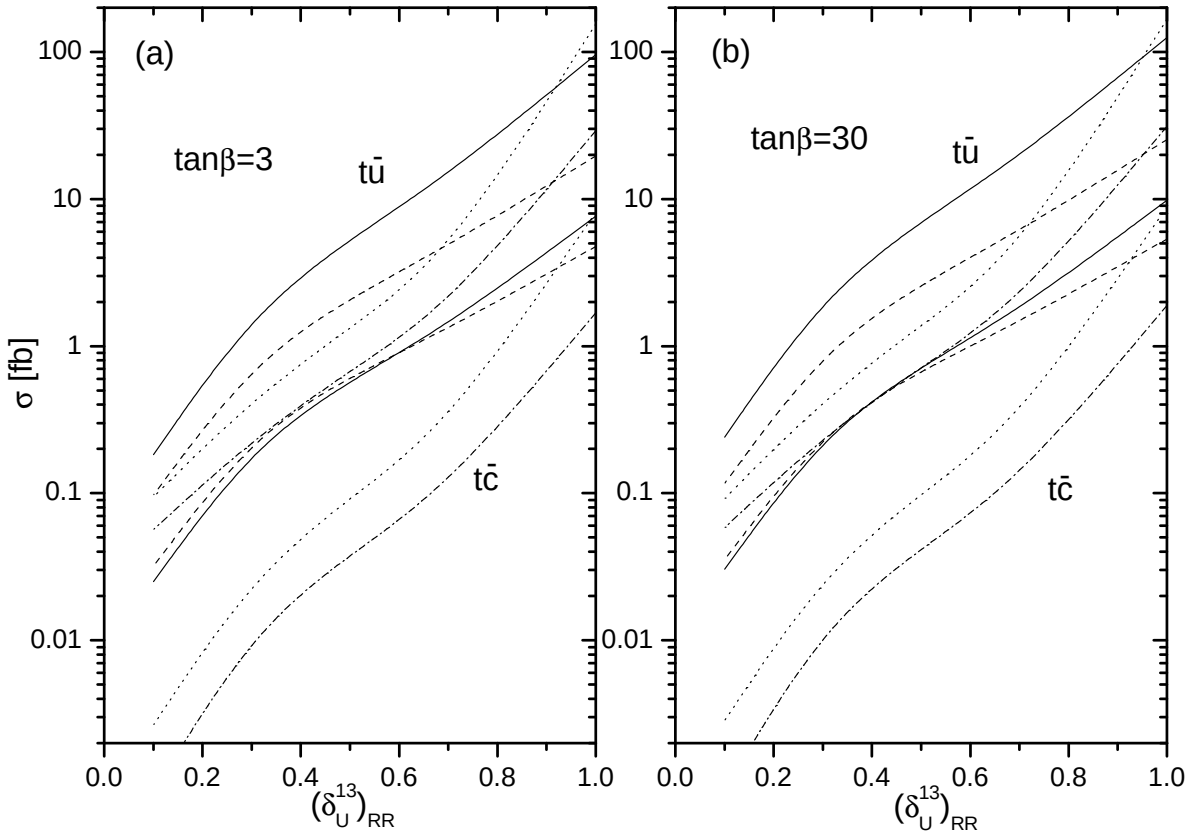

Figure 5: The total cross sections for the $pp \to t\bar{c}(\bar{u})$ with RR off-diagonal elements $(\delta_U^{13})_{RR}$. Here, solid line: $m_{\tilde{g}} = 200$ GeV, $M_{\rm SUSY} = 400$ GeV; dashed line: $m_{\tilde{g}} = 300$ GeV, $M_{\rm SUSY} = 400$ GeV; dotted line: $m_{\tilde{g}} = 200$ GeV, $M_{\rm SUSY} = 1000$ GeV; dash-dotted line: $m_{\tilde{g}} = 300$ GeV, $M_{\rm SUSY} = 1000$ GeV.

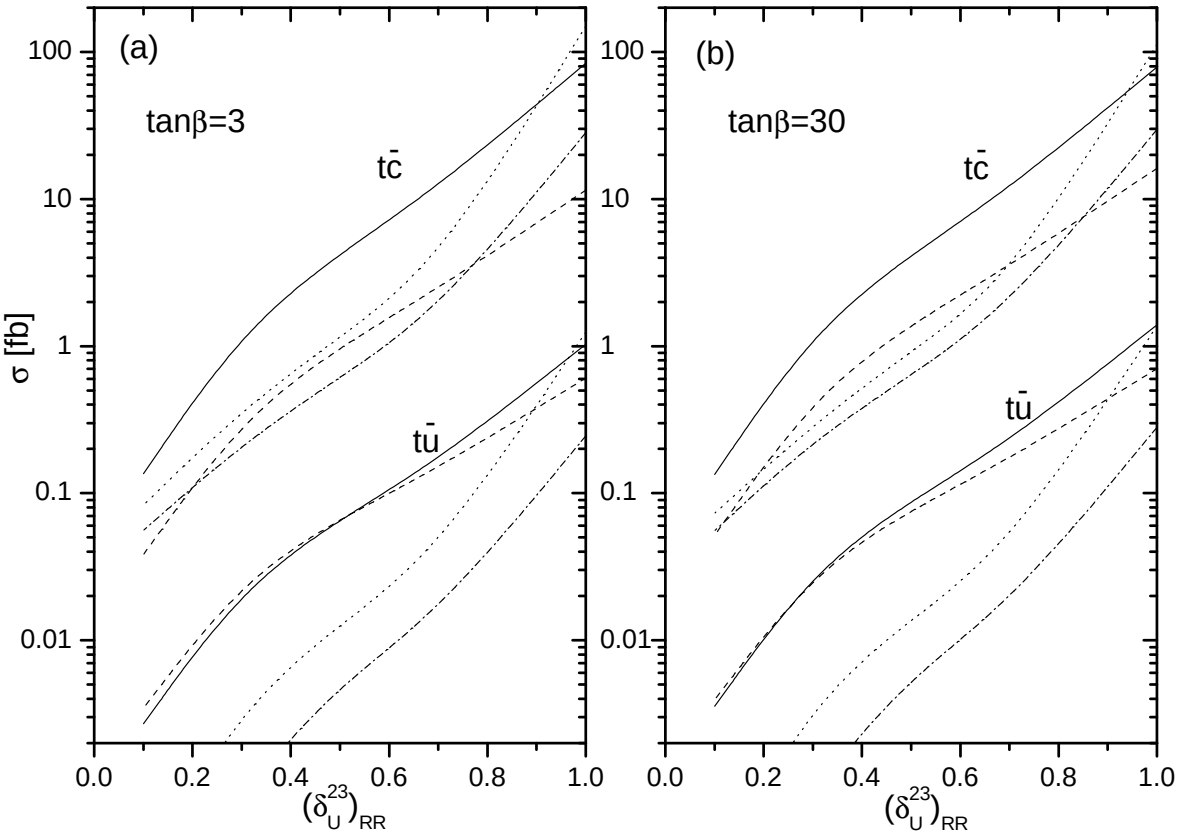

Figure 6: The total cross sections for the $pp \to t\bar{c}(\bar{u})$ with RR off-diagonal elements $(\delta_U^{23})_{RR}$. Here, solid line: $m_{\tilde{g}} = 200$ GeV, $M_{\rm SUSY} = 400$ GeV; dashed line: $m_{\tilde{g}} = 300$ GeV, $M_{\rm SUSY} = 400$ GeV; dotted line: $m_{\tilde{g}} = 200$ GeV, $M_{\rm SUSY} = 1000$ GeV; dash-dotted line: $m_{\tilde{g}} = 300$ GeV, $M_{\rm SUSY} = 1000$ GeV.

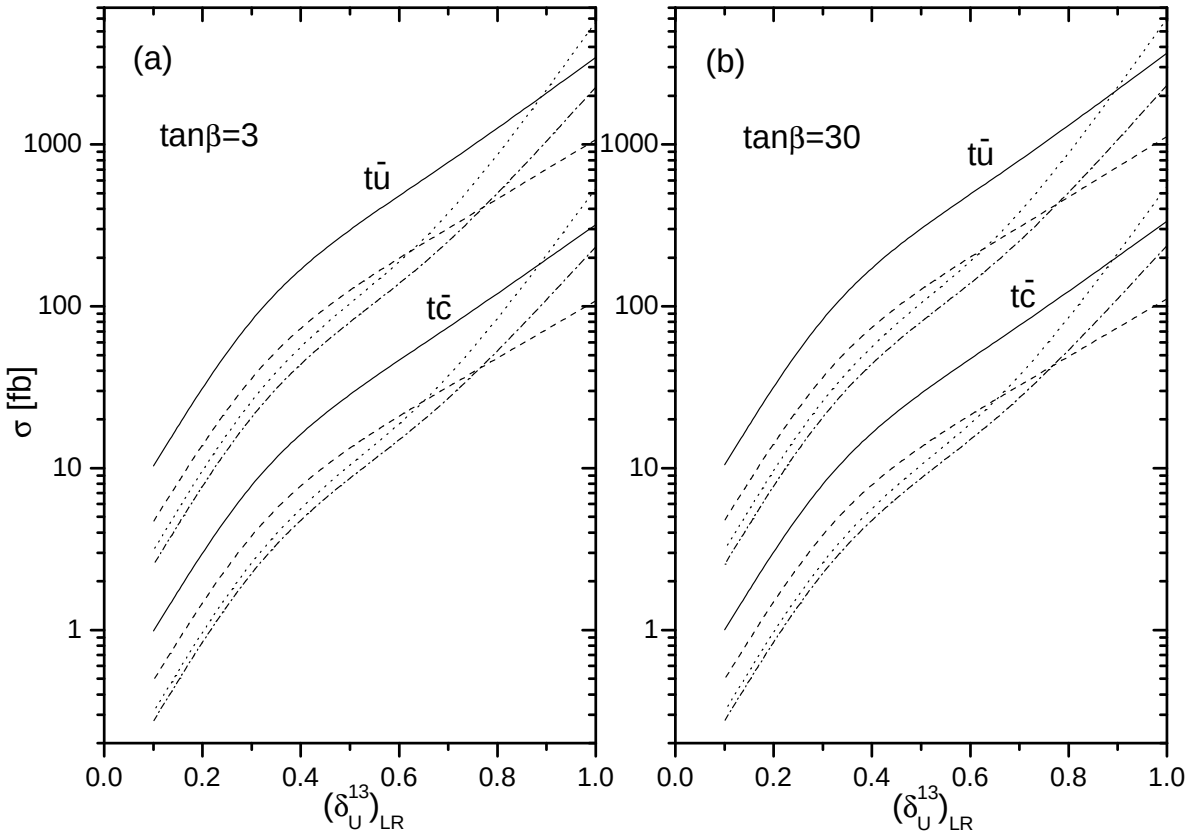

Figure 7: The total cross sections for the $pp \to t\bar{c}(\bar{u})$ with LR off-diagonal elements $(\delta_U^{13})_{LR}$. Here, solid line: $m_{\tilde{g}} = 200$ GeV, $M_{\rm SUSY} = 400$ GeV; dashed line: $m_{\tilde{g}} = 300$ GeV, $M_{\rm SUSY} = 400$ GeV; dotted line: $m_{\tilde{g}} = 200$ GeV, $M_{\rm SUSY} = 1000$ GeV; dash-dotted line: $m_{\tilde{g}} = 300$ GeV, $M_{\rm SUSY} = 1000$ GeV.

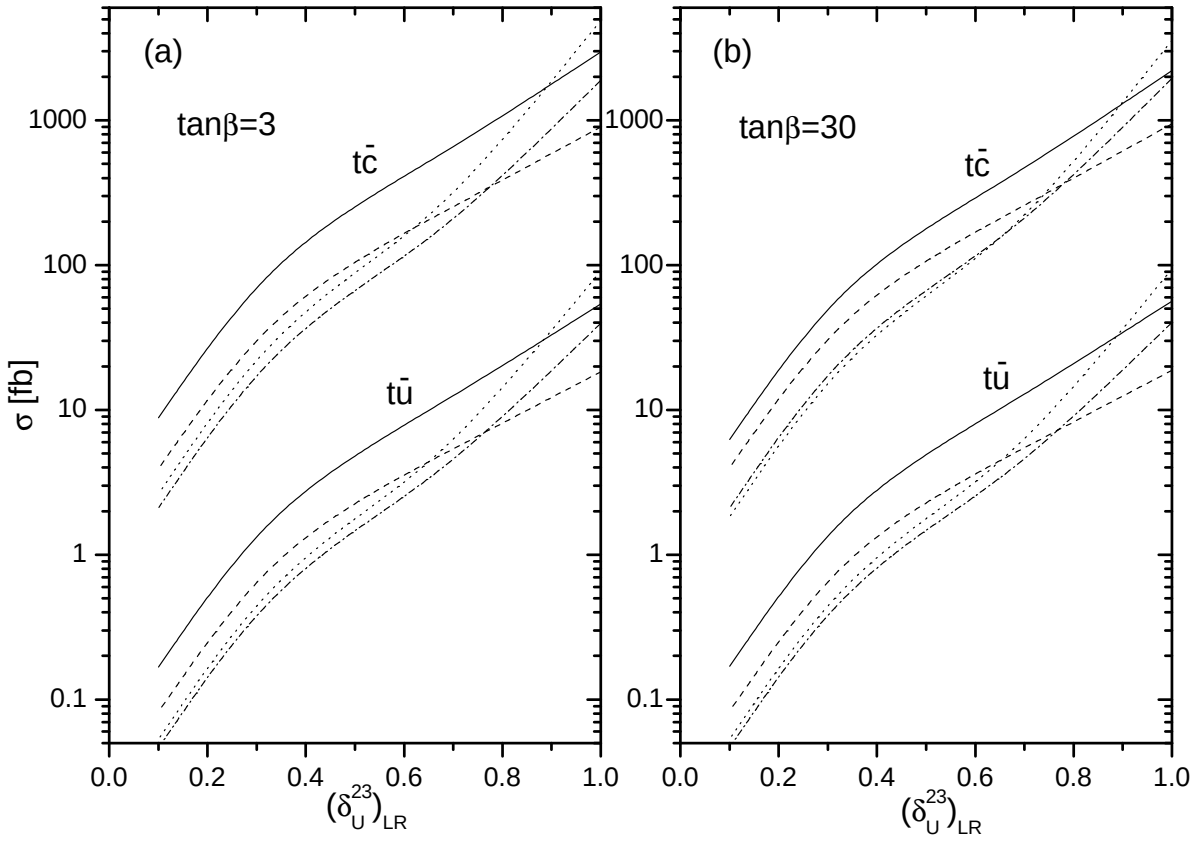

Figure 8: The total cross sections for the $pp \to t\bar{c}(\bar{u})$ with LR off-diagonal elements $(\delta_U^{23})_{LR}$. Here, solid line: $m_{\tilde{g}} = 200$ GeV, $M_{\rm SUSY} = 400$ GeV; dashed line: $m_{\tilde{g}} = 300$ GeV, $M_{\rm SUSY} = 400$ GeV; dotted line: $m_{\tilde{g}} = 200$ GeV, $M_{\rm SUSY} = 1000$ GeV; dash-dotted line: $m_{\tilde{g}} = 300$ GeV, $M_{\rm SUSY} = 1000$ GeV.

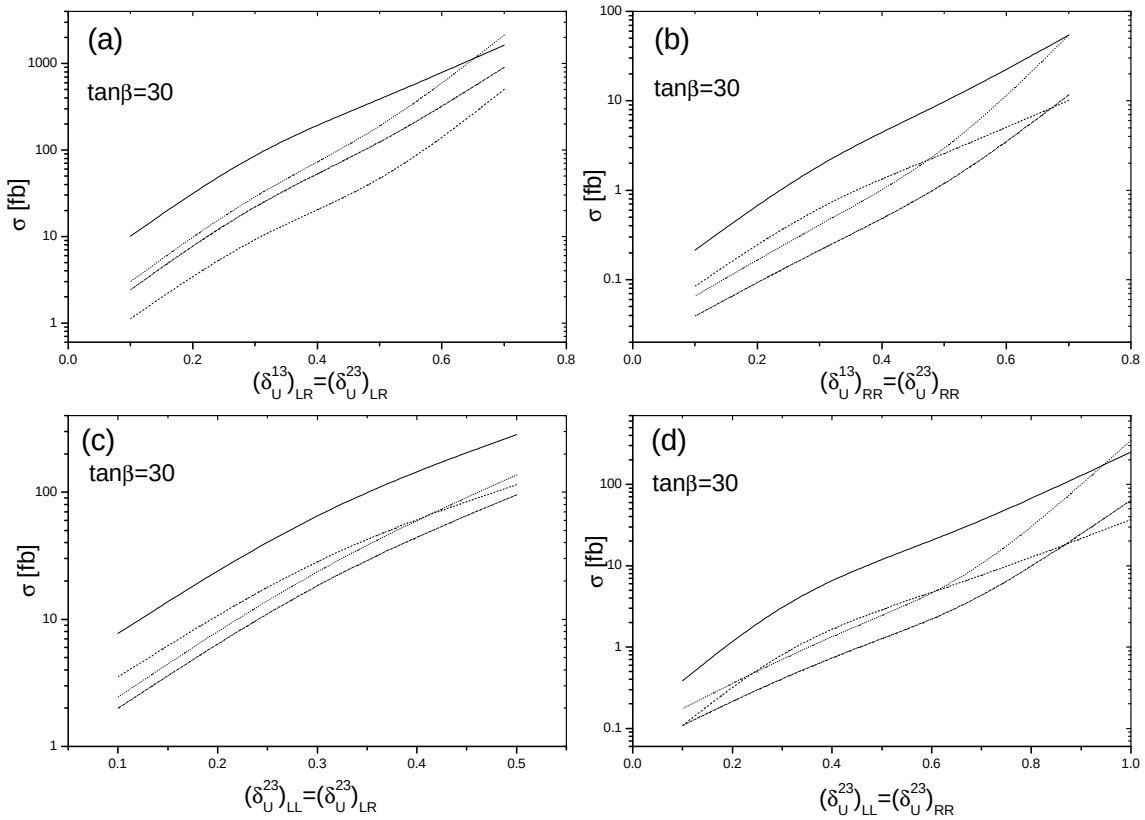

Figure 9: Typical interference effects between different matrix elements within one block in (a) and (b), and between different blocks in (c) and (d). Here, solid line: $m_{\tilde{g}} = 200$ GeV, $M_{\rm SUSY} = 400$ GeV; dashed line: $m_{\tilde{g}} = 300$ GeV, $M_{\rm SUSY} = 400$ GeV; dotted line: $m_{\tilde{g}} = 200$ GeV, $M_{\rm SUSY} = 1000$ GeV; dash-dotted line: $m_{\tilde{g}} = 300$ GeV, $M_{\rm SUSY} = 1000$ GeV.

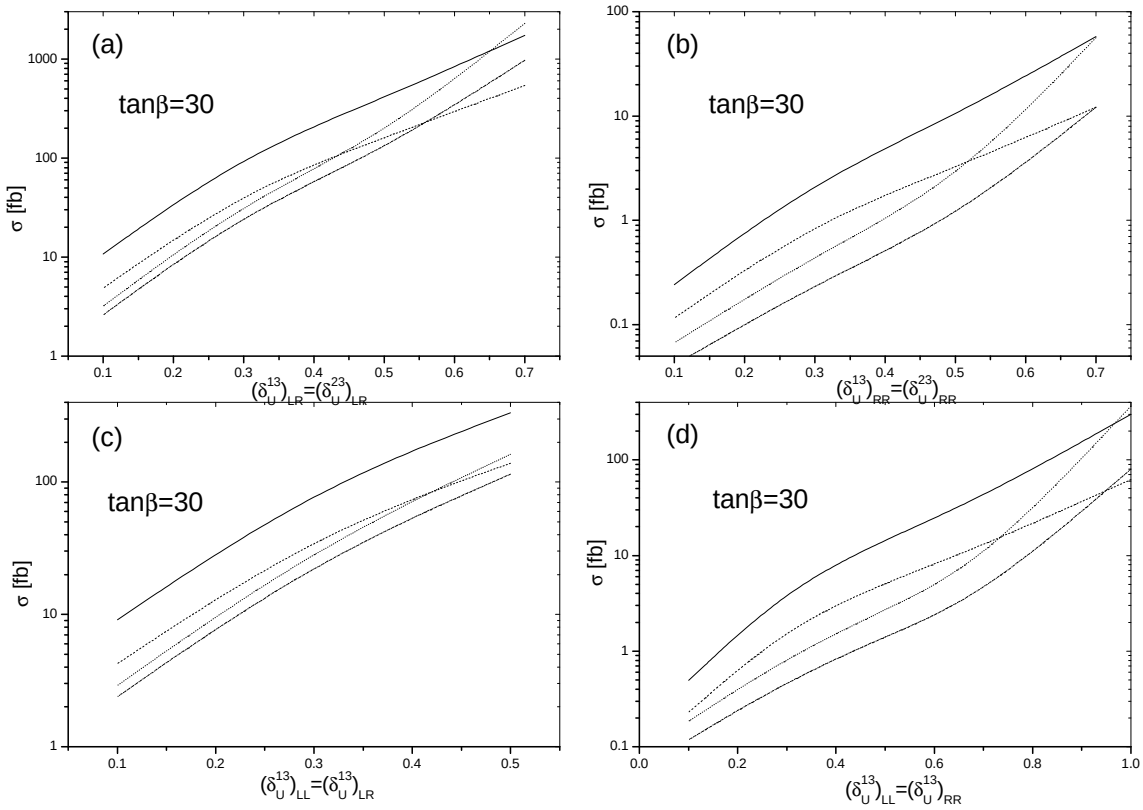

Figure 10: Similar as Fig.9, but for $t\bar{u}$.